Construction and Building Materials

Optimisation of hybrid eco-efficient mortars with aggregates from construction and demolition waste and olive biomass ash

--Manuscript Draft--

Manuscript Number:	CONBUILDMAT-D-23-05062R1
Article Type:	Research Paper
Keywords:	olive Biomass Bottom Ash, Construction and Demolition Waste, Mixed Recycled Aggregates, cement mortars.
Corresponding Author:	Francisco Agrela, Ph.D. University of Cordoba Cordoba, Córdoba SPAIN
First Author:	Manuel Rosales
Order of Authors:	Manuel Rosales
	Francisco Agrela, Ph.D.
	M.I. Sánchez de Rojas
	M. Cabrera
	Julia Rosales
Abstract:	Materials considered as waste, such as Construction and Demolition Wastes (C&DW) and Biomass Bottom Ash (BBA) are the subject of this study to implement them in cement-based materials. After basic and advanced characterization, as well as leaching studies to assess the environmental impact, they are implemented in mortars as a replacement for standard silica sand. In this way, their mechanical behaviour, durability and micro-properties in hardened state are tested. The feasibility of implementing Mixed Recycled Aggregates (MRA) from C&DW and BBA to replace natural sand in high substitution rates is studied by substituting the wastes alone and in combination. Mortar mixes in which 50% of the aggregate is replaced, reaching more than 80% of the standard mortar strength. Mixtures in which 10% of the aggregate is replaced reaching more than 95% of the standard mortar strength.
Suggested Reviewers:	Victoria Borrachero vborrachero@cst.upv.es She is a specialist in the study of the application of different wastes in construction materials. She has countless studies of alkaline activation of materials
	Cesar Medina cmedinam@unex.es He is expert in the study of industrial waste for its use in civil infrastructure. He is highly specialized in the study of the mechanical durability and properties
	Valeria Corinaldesi v.corinaldesi@staff.univpm.it She is a specialist in studies of advanced composite materials based on cement for structural and design applications, paying special attention to aspects of performance and sustainability.
	Chi Sun Poon cecspoon@polyu.edu.hk He´s research interests include developing functional practices of reusing and recycling of construction secondary materials in the manufactured of concrete. He specifically works on waste evaluation and interpretation of data from environmental assessment tests.
	Belen Gonzalez Fonteboa bfonteboa@udc.es She is a specialist in the study of the application of different wastes in construction materials. She has countless studies of alkaline activation of materials.

Optimisation of hybrid eco-efficient mortars with aggregates from construction and demolition waste and olive biomass ash

M. Rosales[1], F. Agrela[1*], M.I. Sánchez de Rojas[2], M. Cabrera[1], J. Rosales[1]

[1] Area of Construction Engineering, University of Cordoba, Cordoba, Spain

[2] Eduardo Torroja Institute for Construction Science, UEX-CSIC Partnering Unit, C/ Serrano Galvache, 28033 Madrid, Spain

Abstract

Materials considered as waste, such as Construction and Demolition Wastes (C&DW) and Biomass Bottom Ash (BBA) are the subject of this study to implement them in cement-based materials. After basic and advanced characterization, as well as leaching studies to assess the environmental impact, they are implemented in mortars as a replacement for standard silica sand. In this way, their mechanical behaviour, durability and micro-properties in hardened state are tested. The feasibility of implementing Mixed Recycled Aggregates (MRA) from C&DW and BBA to replace natural sand in high substitution rates is studied by substituting the wastes alone and in combination. Mortar mixes in which 50% of the aggregate is replaced, reaching more than 80% of the standard mortar strength. Mixtures in which 10% of the aggregate is replaced reaching more than 95% of the standard mortar strength.

Keywords: olive Biomass Bottom Ash, Construction and Demolition Waste, Mixed Recycled Aggregates, cement mortars.

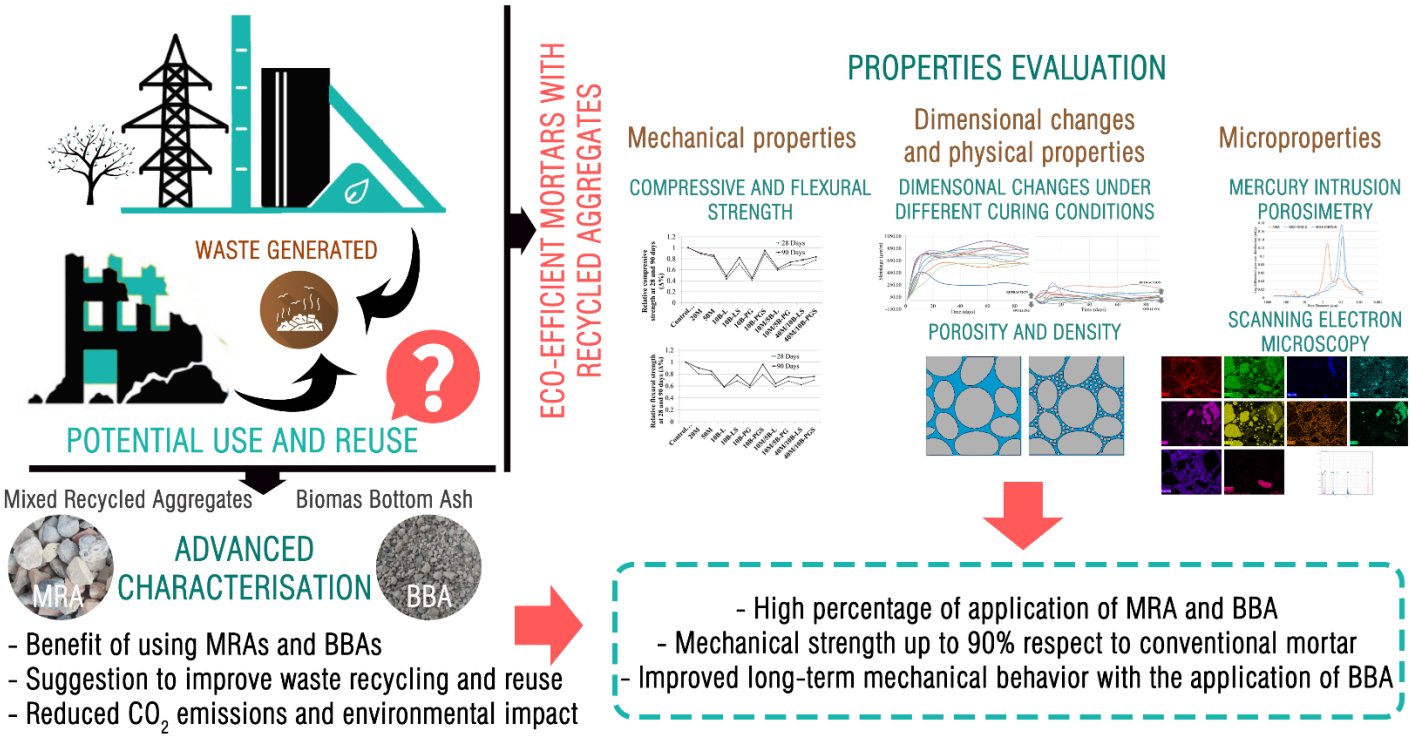

1. Introduction

Advancement in the generation of new materials such as cement mortars made mainly from waste as a substitute for traditional raw materials is fundamental towards mitigating excessive energy consumption, consumption of natural resources, carbon dioxide emissions and environmental degradation, and therefore leading to a reduction in climate change.

Today, the management of waste generated by human activity is of great interest. This management is directly related to sustainable development, based on the 17 Sustainable Development Goals. (SDGs) promoted by The 2030 Agenda for Sustainable Development, adopted by all United Nations Member States [1], especially goal 11: sustainable cities and communities, and goal 12: responsible production and consumption, closely related to goal 13: climate action. The waste derived from the remodelling of buildings (Construction & Demolition Wastes) and the waste derived from the generation of electric energy through the burning of forest biomass (Olive Biomass Bottom Ashes) is substantial.

In Europe, currently, a large amount of construction and demolition waste (CDW) is produced. This figure amounted to 372 Mt, excluding excavated soils, in 2020 [2], which represents almost 40% of the overall waste generated in Europe [3].The construction sector is responsible for 30% of total waste in the world [4], and in addition to generating large amounts of waste it is responsible for high consumption of natural resources and energy. It is a sector that traditionally has a linear approach, where natural raw materials are used, manufactured and then destroyed at the end of their useful life and accumulated in landfills. This linear production produces large amounts of CO_2 emissions, with the construction sector being responsible for 23% of carbon dioxide emissions from global economic activities [5, 6].

Advancing towards a circular economy and proper management of natural resources includes obtaining energy through renewable sources as a substitute for fossil fuels. Electricity production through biomass accounted for 5.1% of total energy consumption in 2018 [7], and the most widely used biomass is forest biomass, accounting for 85% of that used for energy purposes [8, 9].

Biomass combustion is considered clean energy, a reason that has led to an increase in the construction of plants [10]. Biomass combustion generates waste called biomass ash, which currently has few recycling alternatives [11].

The use of this waste is focused on the substitution of natural elements for construction related materials, the main subject of this document. By including such waste in construction elements, two benefits are achieved. The first is to avoid the accumulation of waste, which has no real use [12] and the second focuses on avoiding the use of naturally occurring materials.

Within construction and demolition waste, mixed recycled aggregates (MRA) are produced and accumulated in large quantities. This material is mainly composed of concrete aggregates and masonry rubble, obtained in the largest quantities in waste treatment plants [13]. MRA as a substitute for natural sand has been studied in different previous works and it should be taken into

account that the workability of the mixes is modified when MRA is introduced, due to the fact that the absorption of this recycled material is different from the absorption of natural sand [14-16]. On the other hand, mixes have been found in which the replacement of natural sand with sand from recycled aggregates have better mechanical behaviour [17, 18], which may be due to the pozzolanic capabilities of the ultrafine MRA, as the ceramic particles have cementitious properties [19, 20].

This pozzolanic capacity has also been demonstrated for biomass bottom ash (BBA). The pozzolanic capacity of BBA depends mainly on its chemical composition, especially on the Si+Fe+Al and CaO content. In addition to the composition, the organic matter content and crystalline structure of the phases should be evaluated as a factor influencing the pozzolanicity of the material [21, 22].

The substitution of natural aggregates by BBA has been studied for the manufacture of concrete and mortar. The basic properties of mortars manufactured with BBA include low density and high porosity materials [23-26]. The high organic matter content of BBA is one of the most restrictive conditions for it to be used in construction materials [27] as organic matter affects durability and mechanical behaviour. However, with proper treatment, sieving, crushing, calcination or washing, the amount of organic matter decreases and the properties of the mortars improve [25].

Therefore, the combination of MRA and BBA as a substitute aggregate for natural aggregate in the manufacture of mortar has a high potential, mainly due to the pozzolanic properties of the material that lead to an increase in mechanical strength [20].

In this study, substitutions between 10-50% of natural aggregate by different combinations of MRA and BBA subjected to simple screening processes have been carried out, as well as an advanced characterisation of each of the materials and subsequently a study of the mechanical, durability and microstructural properties of the mortars manufactured with high substitution percentages.

2. Materials

2.1. Characterisation properties of materials

2.1.1. Cement

The cement used in this research was CEM I 42.5R, and the physicochemical properties are summarised in Table 1.

Table 1. Physicochemical properties of Cement CEM I 42.5R

	FRX (%)										UNE-EN 196-1 [28]
	CaO	SiO_2	SO_3	Al_2O_3	Fe_2O_3	MgO	K_2O	Na_2O	TiO_2	LOI	Density (kg/m^3)
CEM I 42.5R	67.92	17.57	4.50	3.32	1.81	1.38	1.07	0.36	0.27	1.80	3.14

The cement used is a type of cement with high compressive strength, especially suitable for mass concrete, reinforced concrete, non-prestressed prefabricated concrete and for the manufacture of mortars in general.

2.1.2. Normalised Sand

Normalised sand according to DIN EN 196-1 [28] is characterised by its particle size distribution. The grain sizes are in the range of 0.08 and 2.00 millimeters. Their proportions are shown in table 2. The maximum moisture content of the sand is 0.2 per cent, marketed in bags weighing 1.350 (± 5) grammes.

Table 2. Particles size distribution.

Sieve (mm)	Lower limit	Interval average	Upper limit
2	0	0	0
1.6	2	7	12
1	28	33	38
0.5	62	67	72
0.16	82	87	92

0.08	98	99	100

Standard sand is produced artificially. For this purpose, natural and quartz-rich sands are screened in several steps to obtain the respective fractions of the different grain sizes.

2.1.3. Mixed Recycled Aggregates

The recycled aggregate used comes from a recycling plant in Cordoba, Andalusia (Spain). It is a company dedicated to waste management, with special emphasis on the management of construction and demolition waste (C&DW).

Table 3 shows the composition of the MRA; the recycled aggregate composition test (performed according to UNE-EN 933-11 [29] is a test of special importance to classify recycled aggregates according to their nature, as well as to provide an index of their quality.

Table 3. Composition of MRA.

Composition MRA (0 – 22 mm) UNE-EN 933-11 [29]						
Concrete (%)	Natural Aggregate (%)	Ceramic (%)	Bituminous (%)	Others (%)	Glass (%)	Floating (cm^3/kg)
43.7	33.8	19.1	2.8	0.6	0	0

It can be observed that it is mainly composed of ceramic materials, concrete and natural aggregates. Depending on the quality of the aggregate, it may also contain certain percentages of impurities such as glass, metals, wood, gypsum, organic soil, etc. These impurities can have a negative influence on the reusability properties of the new material and must therefore be limited, but the MRA used in the study has no relevant impurity percentages.

Table 4 shows the chemical composition of the MRA, in which it can be observed that it is chemically formed by silica oxide (44.63 %), calcium oxide (34.19 %), aluminium oxide (9.42 %) followed by other oxides in a smaller proportion (< 4%). The chemical composition varies according to the place of origin and the type of treatment given at the plant. Previous studies showed CDW powder with high Al_2O_3 and Fe_2O_3 content [30]. The MRAs analysed in this study resulted in lower values of both components, as shown in the study by Medina et al. [31].

It is important to note that the CaO content is higher than that observed in other recycled aggregates studied [32, 33].

Table 4. Constituents of MRA (FRX).

Constituents (%) BBA-PG (0 – 4 mm) UNE-EN 933-11 [29]											
CaO	SiO_2	K_2O	Al_2O_3	MgO	P_2O_5	Fe_2O_3	SO_3	Na_2O	TiO_2	MnO_2	LOI
33.62	43.88	2.01	9.26	3.19	0.21	3.11	1.75	0.61	0.53	0.14	1.69

Table 5 shows a summary of the physical and chemical properties that were evaluated for the MRA. The values correspond to the average of three samples taken from the material.

Table 5. Physic-chemical properties of different fractions of MRA.

Properties	CHARACTERIZATION MRA		
	Size	Results	Test Method
Density-SSD (kg/m^3)	0 - 4 mm	2.35	UNE-EN 1097-6 [34]
Water Absortion (%)	0 - 4 mm	9.52	
Friability Ratio (%)	0.1 - 2 mm	23.4	UNE 146404 [35]
Sand Equivalent (%)	0 - 2 mm	75.87	UNE-EN 933-8 [36]
Organic Content (%)	0 - 2 mm	0.21	UNE 103204 [37]
Chlorides (%)	0 - 2 mm	0.08	UNE-EN 1744-1 [38]
Water-soluble sulfates (%)	0 - 2 mm	0.38	
Acid-soluble sulfates (%)	0 - 2 mm	0.38	

According to previous studies, an important property that determines the use of MRA in different applications is the density and absorption of the aggregate. There are studies [13] in which the limits of these properties are established according to different standards. According to the most restrictive standard, the MRA density must be higher than 2.2 kg/m3 and the water absorption lower than 7%. As shown in Table 5, the MRA analysed presented higher density values; however, due to the high content of ceramic particles, the absorption of the material was higher. The fine fraction of the material resulted in higher absorption values, which is similar to the one obtained in the study [39], showing water absorption values of 8% in the fine fraction and 5% in the coarse fraction.

Parameters such as friability, Los Angeles coefficient or sand equivalent that evaluate the erosion

resistance of the material showed values of 23.4, 34.72 and 75.87 respectively. These values indicate that the MRA studied showed better properties with respect to previous studies in which the results of friability ratios for different MRA studied [40] were between 24.02% and 27.20%, or another study [41] in which the friability ratio was 23.94% for recycled aggregates.

In relation to the Los Angeles results, [42] this study gives three different numbers for three different recycled aggregates. These Los Angeles results are 38%, 29% and 42% for recycled concrete, ceramics and mixed debris respectively. Other studies [43] present values of Los Angeles 38.1% for recycled concrete aggregates and 44.2% for recycled masonry. Concerning this paper [44] on the MRA from the pavement of Lisbon International Airport, the results of the Los Angeles test showed values of between 36% and 45%.

There is a study [45] that includes a characterisation of MRA where Los Angeles is 40.99% and the constituents are 44.11% for concrete and 33.56% for ceramics. The value of concrete in MRA is 45.64% and the value of ceramics (clay-based material) is 5.3%. Regarding the quantity of natural aggregate, this value is 28.06%. [31]

2.1.4. Olive Biomass Bottom Ash from Puente Genil (BBA-PG)

Biomass ash was extracted from a combined cycle cogeneration (13 + 4.4 Megawatt -MW-) and biomass power generation (9.6 MW) industrial complex located in Puente Genil, Cordoba (Andalusia, Spain).

The biomass used as fuel for the plant comes mainly from oil cake (waste obtained from the olive pomace oil extraction process) but also olive pruning residues, almond shells, cotton and sunflower stubble, forestry residues, etc., from crops in the area.

The chemical composition of the ash samples from Puente Genil was determined by X-ray fluorescence (XRF) and is presented in Table 6.

Table 6. Constituents of BBA-PG (FRX).

Constituents (%) BBA-PG (0 – 4 mm) UNE-EN 933-11 [29]											
CaO	SiO_2	K_2O	Al_2O_3	MgO	P_2O_5	Fe_2O_3	SO_3	Na_2O	TiO_2	MnO_2	LOI
46.72	24.38	9.07	4.89	4.19	4.16	5.25	0.38	0.55	0.28	0.09	3.92

The main oxides found in the ash were CaO, SiO_2, and Al_2O_3, consistent with other studies [21], [46], which are in turn the major components in Portland cement [47]. The ash had a $SiO_2+Al_2O_3+Fe_2O_3$ content < 70%. It is a high lime content ash, as its CaO content exceeds 45%, with possible hydraulic and/or pozzolanic properties. However, it is worth noting the presence of alkalis in its composition (K_2O > 10%) which can negatively affect the durability of the material.

Table 7 shows a summary of the physical and chemical properties that were evaluated for the BBA-PG.

Table 7. Physic-chemical properties of different fractions of BBA-PG

Properties	CHARACTERIZATION BBA-PG		
	Size	Results	Test Method
Density-SSD (kg/m^3)	0 - 4 mm	2.01	UNE-EN 1097-6 [34]
Water Absortion (%)	0 - 4 mm	19.5	
Friability Ratio (%)	0.1 - 2 mm	24.9	UNE 146404 [35]
Sand Equivalent (%)	0 - 2 mm	69.83	UNE-EN 933-8 [36]
Organic Content (%)	0 - 2 mm	3.31	UNE 103204 [37]
Chlorides	0 - 2 mm	0.25	UNE-EN 1744-1 [38]
Water-soluble sulfates (%)	0 - 2 mm	0.19	
Acid-soluble sulfates (%)	0 - 2 mm	0.19	

Regarding the water absorption of BBA-PG, values close to 20% were observed, due to the fact that the ash is formed by highly porous and rough textured particles [48], [49]. Organic matter values below 3.5% were detected, whose value depends mainly on the combustion technology of each power plant [50]. The resistance to fragmentation, due to its structure, presents high values of friability compared to natural sand [51], and the soluble sulphate contents are below the limits set by the regulations for a natural aggregate.

2.1.1. Olive Biomass Bottom Ash from Linares (BBA-L)

In this work, biomass bottom ash from a Linares biomass combustion power plant has been studied. This power plant is situated in the Andalusia region (Spain), in which there is a high concentration of olive orchards.

In relation to chemical composition (Table 8), the BBA-L is composed mainly of SiO_2, CaO and K_2O. Similar results were found in previous studies [11, 52].

Table 8. Constituents of BBA-L (FRX).

Constituents (%) BBA-L (0 – 4 mm) UNE-EN 933-11[29]											
CaO	SiO_2	K_2O	Al_2O_3	MgO	P_2O_5	Fe_2O_3	SO_3	Na_2O	TiO_2	MnO_2	LOI
30.63	32.75	14.85	6.40	4.88	2.95	2.92	0.49	0.33	0.25	0.14	3.41

Table 9. Physic-chemical properties of different fractions of BBA-L.

Properties	CHARACTERIZATION BBA-L		
	Size	Results	Test Method
Density-SSD (kg/m^3)	0 - 4 mm	1.89	UNE-EN 1097-6 [34]
Water Absortion (%)	0 - 4 mm	19.8	
Friability Ratio (%)	0.1 - 2 mm	36.5	UNE 146404 [35]
Sand Equivalent (%)	0 - 2 mm	67.42	UNE-EN 933-8 [36]
Organic Content (%)	0 - 2 mm	2.49	UNE 103204 [37]
Chlorides (%)	0 - 2 mm	0.22	UNE-EN 1744-1 [38]
Water-soluble sulfates (%)	0 - 2 mm	0.3	
Acid-soluble sulfates (%)	0 - 2 mm	0.3	

In table 9, it can be observed that BBA-L presents great facility for fragmentation, being able to obtain powder easily. In addition, once the water absorption tests have been carried out, we find that the results present significantly higher absorptions than natural aggregate. This parameter is of great importance for construction because concrete and mortars with excess or insufficient water behave worse mechanically. Determine the amount of water necessary to saturate the BBA and thus leave sufficient hydration water for pozzolanic reactions. is a critical point in these additions

of residues in construction materials [53].

The density result of the BBA-L showed lower values compared to a natural aggregate, directly related to the absorption, which resulted in high values. Similar results were obtained in previous studies, where the characterisation of BBA with different origins showed density values between 1.7 and 2.5 kg/m^3 and very high and variable absorptions between 19-28% [23, 25, 54-56].

Figure 1 shows the granulometry test for MRA, BBA-PG and BBA-L.

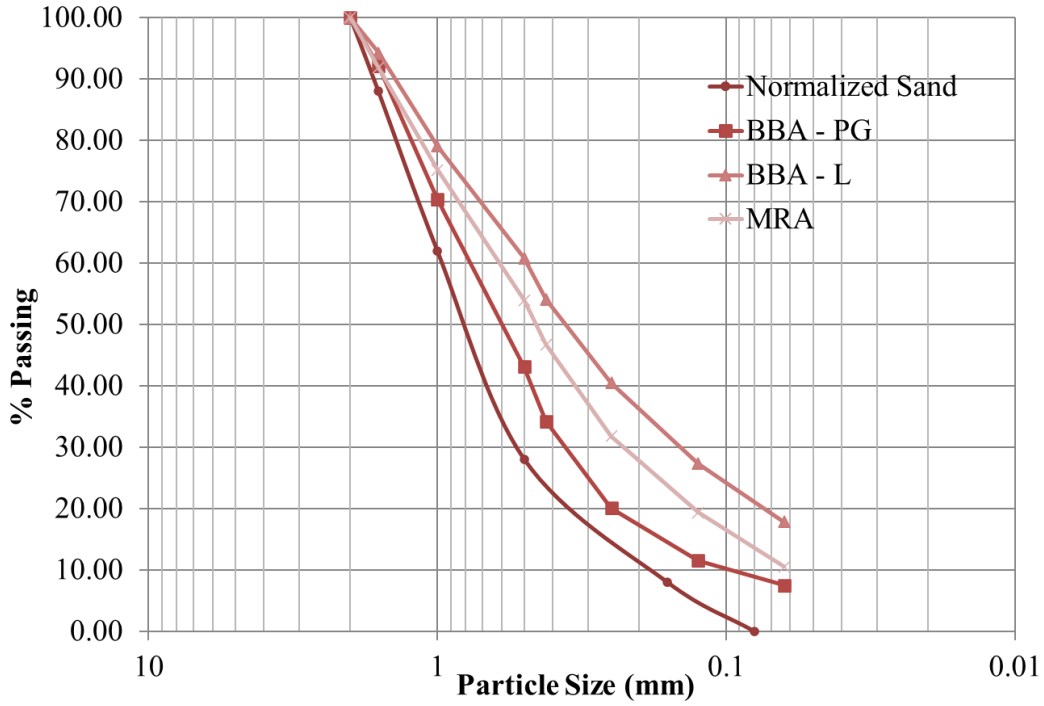

Figure 1. Particle size distribution of MRA, BBA-PG and BBA-L

2.1.2. Determination of the reactivity of aggregates. UNE 146513:2018 [57]. ASR and ACR

The alkali-aggregate reaction involves chemical interactions between the alkaline hydroxides, which usually, but not always, come from the cement used in the manufacture of concrete, and the reactive components of the aggregates used [58]. Depending on the nature of the aggregates, two different types of reaction have been distinguished: if the aggregates are carbonaceous, the so-called alkali-carbonate reaction occurs, while if the aggregates are of a siliceous nature, the alkali-silica reaction occurs. Figure 2 shows the reactivity results of MRA, BBA-PG and BBA-L.

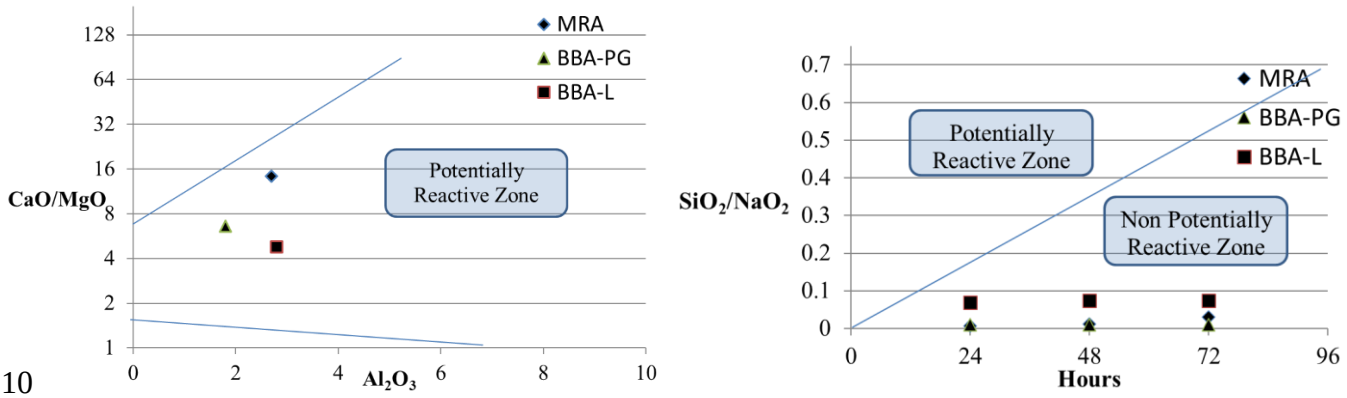

Figure 2. Carbonates test of MRA, BBA-PG and BBA-L

In the figure where Alkali-carbonate reaction (ACR) results are showed, it observes that the three materials are in potentially reactive zone.

Regarding alkali-silica reactions in recycled aggregates, the presence of residual mortar releases some alkalis into the pore solution and increases the risk of reaction. The alkali-silica reaction (ASR) is considered one of the most common degrading agents causing expansion arising from the formation of a gel that swells on contact with water [59]. In the case of BBA, the alkali-silica reaction is mainly due to the potassium content present in both samples [60].

2.2. Environmental leaching study. Compliance Test. UNE-EN 12457-3:2004 [61].

Conformance testing was performed to determine whether the material complies with a specific behaviour or with specific reference values. The tests focus on a number of variables and leaching behaviour previously identified in the basic characterisation tests.

The material was tested in a granular state in contact with deionised water subjected to mechanical agitation at a liquid/solid (L/S) ratio (10 l/kg) for 24 hours.

The results obtained were compared with the legal limits imposed by the EU Landfill Directive (Directive 2003/33) and the material was classified as inert, non-hazardous or hazardous waste (Figure 3).

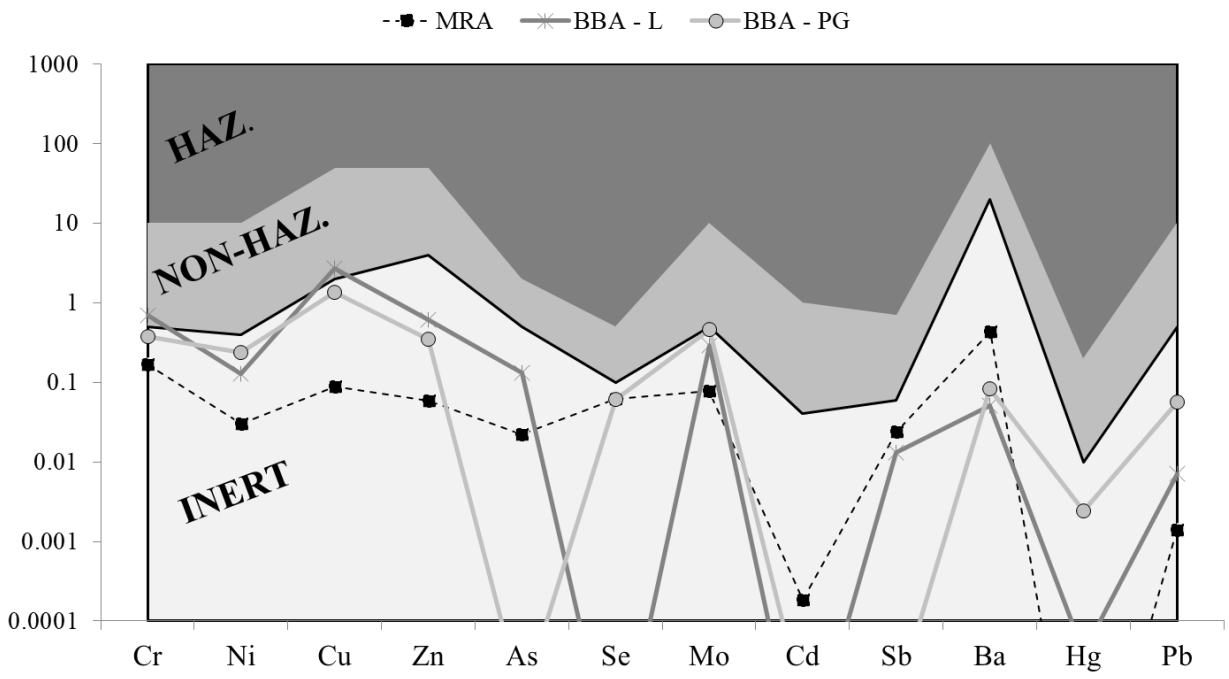

Figure 3. Leaching results.

According to the data presented in Figure 3, the MRA was categorised as inert waste; however, the BBA-L exceeded the legal limit for inert heavy metals: Cr and Cu, and the BBA-PG for Mo. The level of Cu in BBA is mainly due to phytosanitary treatments; copper sulphate is commonly used to combat the fungus Verticillium dahliae which causes the disease commonly known as Verticillium in olive trees [62], while cupric hydroxide is used to treat olive and/or grape diseases called Plasmopara viticola [63]. There are three points that exceed the limits of inert classification, addressing the zone of non-hazardous material. These points are for BBA-L on the elements Cr and Cu and BBA-PG on the element Mo. Note that, although they enter the non-hazardous material zone, these leaching points are located almost on the dividing line between the inert material zone and the non-hazardous material zone.

2.3.Advanced characterisation of the processed materials

This section presents the characterisation of the microcomposition of the waste. Tests such as X-ray diffraction (XRD), thermogravimetric analysis (TGA) and Fourier Transform Infrared

Spectroscopy (FTIR) provide results on the mineralogy of the residues. Moreover, they provide information on the existing organic matter or water, either in the form of moisture or as part of the minerals, called hydrological water.

2.3.1. X-ray diffraction

The study of the x-ray diffraction of each of the materials shows distinct patterns. First, Figure 4 shows the diffractogram of the MRA. This material showed a crystalline structure with marked peaks of Quartz, Calcite and Dolomite. These results are similar to those obtained in previous studies [20, 64].

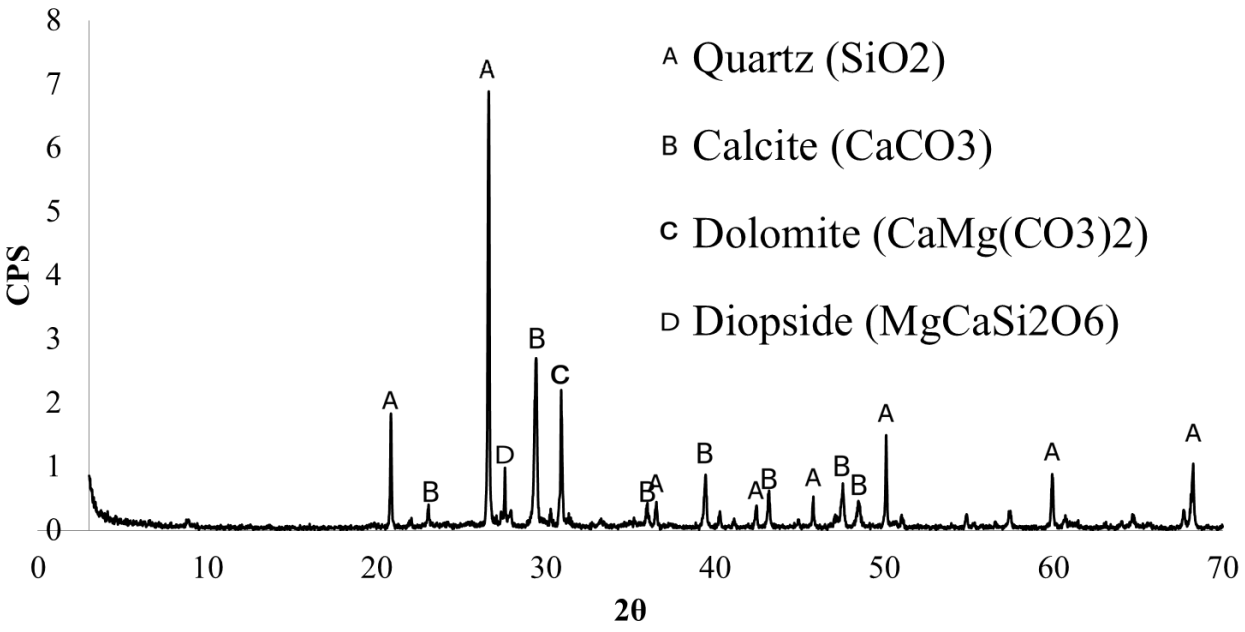

Figure 4. XRD of MRA

Regarding the olive biomass ash, a slightly more amorphous structure than that presented by MRA was observed in both diffractograms (Figure 4 and Figure 5). The BBA showed a composition of quartz, calcite and dolomite crystals mainly, as did MRA; however, the presence of silicates was also observed in this material.

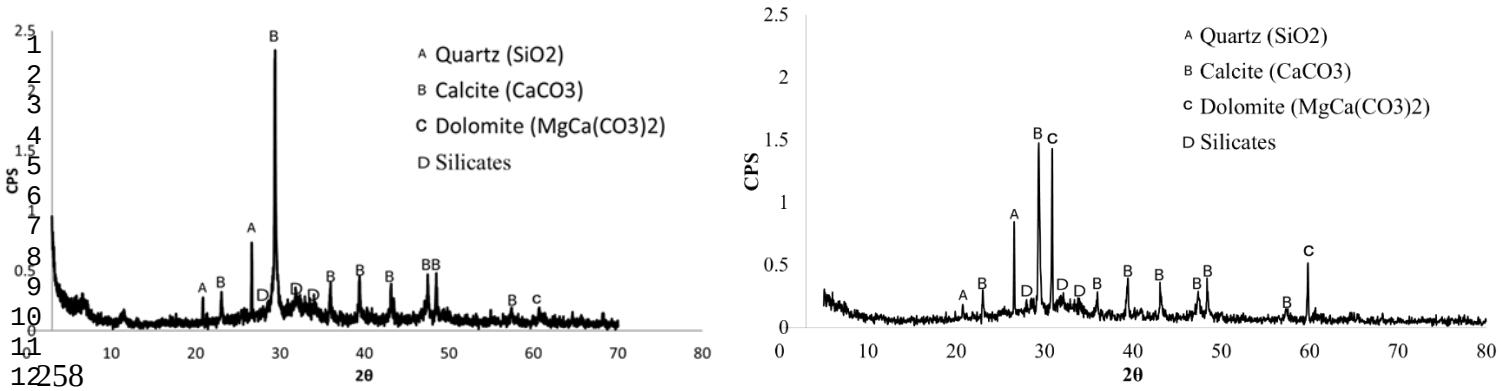

Figure 5. XRD of BBA-PG and BBA-L

Similar compositions were obtained in previous studies in which olive BBA was analysed [25, 46, 54, 56, 65, 66]. The heating process to which the biomass is subjected in energy production is responsible for the high amount of quartz and calcite [67]. As shown in previous studies [46, 68], the presence of silicate crystals in the BBA favours the interaction with the cementitious matrix during setting, which may improve the mechanical strength of the material.

Both types of ash showed similar diffraction, differing in the higher quartz content present in the BBA-L.

2.3.2. Fourier-transform infrared spectroscopy (FTIR)

Fourier-transform infrared spectroscopy shows the absorption of infrared rays of different wavelengths. Thanks to this analysis, we can corroborate the minerals that make up the analysed material. Figure 6. FTIR spectra for MRA, BBA – PG and BBA - L shows the results. After the analysing the figure, we find important peaks that provide a comprehensive analysis of the results. The main peaks are shown in table 10.

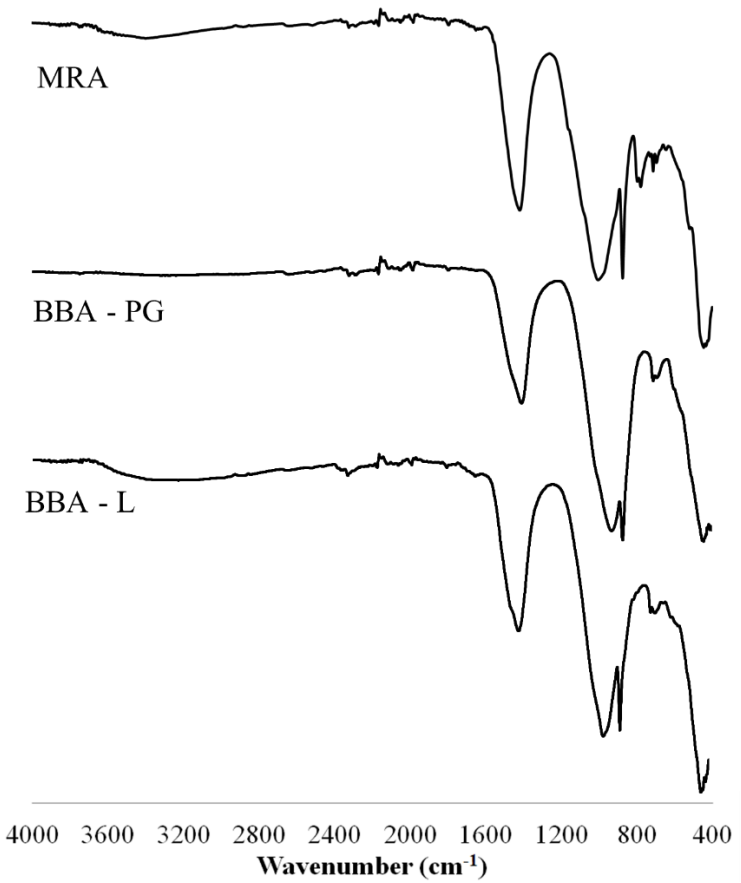

Figure 6. FTIR spectra for MRA, BBA-PG and BBA-L

Table 10. Principal infrared absorption bands

	Wavenumbers cm^{-1}										
MRA	1418	1004	847	795	778	728	712	694	643	519	445
BBA – PG	1413	962	873	711	686	641	440				
BBA - L	1409	930	872	710	691	442					

For peaks found in MRA in wavenumber between 1000 cm^{-1} and 1060 cm^{-1} is related to the presence of asymmetric stretching of Si-O-Si. For BBA-PG and BBA-L, peaks between 950 cm^{-1} and 980 cm^{-1} were found, related with the presence of Si-O-Na, Si-O-K or Si-O-Li stretching since the presence of K in both materials was determined by X-ray fluorescence (Table. 6 and Table 8).

Three materials showed vibrations between 845 cm^{-1} and 880 cm^{-1}, where it is found Si-O stretching and OH bending (Si-OH). For MRA, asymmetric stretching of Si-O-Si were found in 700 cm^{-1} [69].

2.3.3. Thermogravimetric analysis (TGA)

This test determines the mass volatilised when a temperature is imposed on the material. Depending on the mass loss at each temperature, we can determine the compound that volatilises, which is part of the original material. The atmosphere in which the test was carried out is N_2. The results are shown in Figure 7 so that on the left axis is the total mass of the sample and on the right axis is specified the difference in mass lost with respect to the mass at the previous temperature.

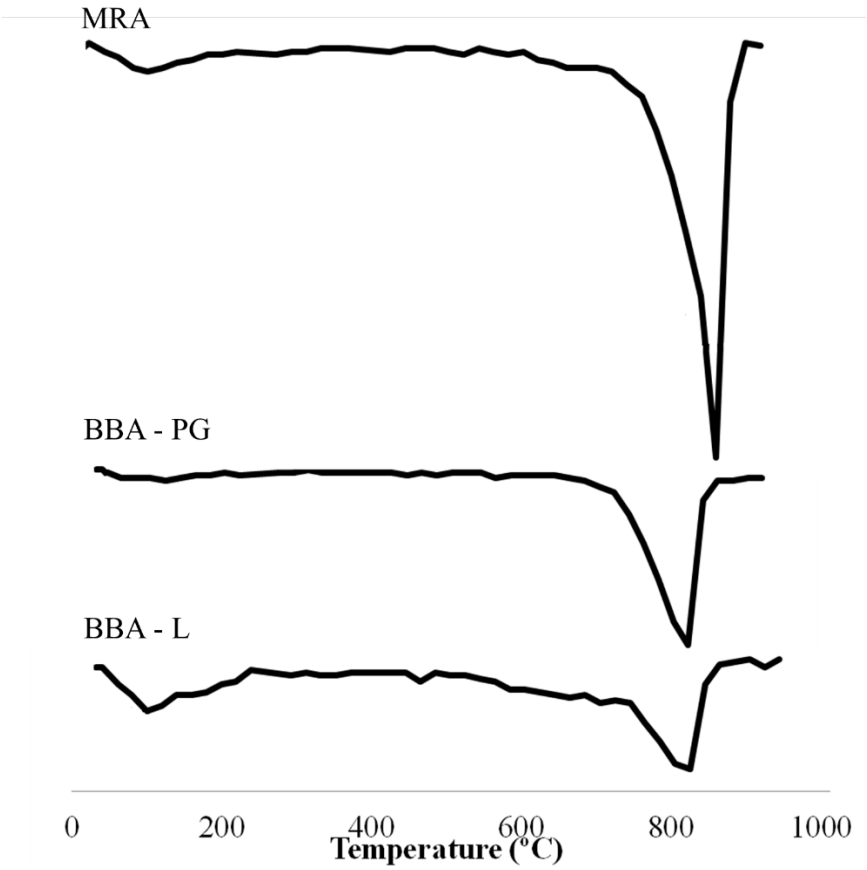

Figure 7. DTGA MRA, BBA-PG and BBA-L

For the MRA and BBA-L samples, a first mass loss peak is found at 101ºC. This mass loss is due to the loss of adsorbed water and water from the SiO_2-CaO. For MRA, water loss at this

temperature can be for the presence of ettringite phases [70]. For MRA it found a peak in temperature of 278ºC determinates a weight loss related with the presence of gibbsite such as Phlogopite [71] and a peak in temperature of 535ºC it found a weight loss related with the presence of Fe_2O_3 and Al_2O_3 hydrated phases from clay minerals [70]. For three samples studied, there was a weight loss of CO_2 from calcite with peak of temperatures around 690, 760 and 840 °C [72, 73]. A big loss of weight appears between 600ºC and 850ºC, where dolomite is decomposed [74].

It can be observed that the mass loss of the biomass bottom ash at 800ºC is more accentuated for the BBA-PG material from Puente Genil with respect to the BBA-L material from Linares. Mass losses at this temperature are related to the existence of carbonate content. As there is a higher mass drop in the bottom ash coming from Puente Genil, this material presents a higher amount of carbonate content due to unburned organic matter, corroborating the data presented in tables 7 and 9 (characterisation of BBA-PG and BBA-L). The results for the amount of organic matter are higher in the BBA-PG (3.31%) than in the BBA-L (2.49%).

3. Mixes proportions, manufacturing and workability

To carry out the mechanical behavior and durability study, 10 mortar mixes were made, including a control mix, with different proportions of natural aggregate replacement by MRA, BBA or a combination of both. It should be noted that the replacements were carried out maintaining the initial volume, so that the densities of the waste were taken into account in comparison with the density of the natural sand.

As observed in the particle size distribution of the material (fig.2), BBA is composed of a large number of fines, which can affect the properties of the manufactured mortars. For this reason, two particle sizes were proposed for the application of BBA; a particle size of the complete fraction (0mm-2mm) named BBA-L and BBA-PG and the removal of particles smaller than 0.125mm by sieving (fraction 0.125mm-2mm) named BBA-LS and BBA-PGS.

Table 11. Mortar mixes dosages.

Mixture No	Mix proportion of the specimen (UNE-EN 196-1 [28])										
	Cement (g)	Normalized Sand (g)	BBA-L (g)	BBA-LS (g)	BBA-PG (g)	BBA-PGS (g)	MRA (g)	Water (g)	Saturation Water (g)	Aditive (ml)	Slump (cm)
Control CEM I 42.5	450	1350	0	0	0	0	0	225	0	0	21.1
20M	450	1080	0	0	0	0	239.73	225	18	2	20.8
50M	450	675	0	0	0	0	599.32	225	38	4	21.0
10B-L	450	1215	99.72	0	0	0	0	225	18	3	20.9
10B-LS	450	1215	0	96.65	0	0	0	225	20	3	21.3
10B-PG	450	1215	0	0	96.14	0	0	225	17	3	21.1
10B-PGS	450	1215	0	0	0	92.56	0	225	17	3	21.1
10M/5B-L	450	1147.5	49.86	0	0	0	119.86	225	20	4	20.4
10M/5B-PG	450	1147.5	0	0	48.07	0	119.86	225	16	4	19.9
40M/10B-LS	450	675	0	96.65	0	0	479.45	225	45	8	20.4
40M/10B-PGS	450	675	0	0	0	92.52	479.45	225	40	8	20.1

During the preparation of the mortar mixes, the consistency of the control mix with CEM I 42.5R and standardized natural sand was taken into account. Because the water absorption of the waste is higher than the absorption of the natural sand, saturation water was included. The saturation water causes the waste to hydrate, thus allowing sufficient water to hydrate the cement and complete the hardening reactions.

In addition, to achieve the consistency of control mortar in the mixes with residues without adding more water than the saturation water, a commercial superplasticiser additive was applied.

4. Methods and Results

After characterising the waste that will replace aggregate in the mortar mixes, this section presents the mortar mixes made, specifying the manufacturing method, workability, mechanical properties, dimensional changes, hardened density and porosity and, finally, micro-properties (MIP and SEM)

of hardened mortars of the mixes with the best mechanical behavior compared to the control mix.

4.1 Mechanical properties- Compressive and flexural strength. UNE-EN 196-1 [28].

In order to study the mechanical behavior of the mortar mixtures, tests were carried out at 2, 7, 28 and 90 days. Three specimens were evaluated for flexural strength and six specimens were evaluated for compressive strength. In addition, table 12 shows the percentage increase in mechanical strength from 28 days to 90 days.

The mechanical strengths of mortars with waste replacing standard natural sand are varied. In the mixtures with low substitutions between 10% and 20% of replacement, it is observed that the replacement of 20% by MRA and the replacement of 10% by BBA from Puente Genil eliminating ultrafine by sieving (10B-PGS) are the ones that present the best mechanical behaviour. The mechanical compressive strengths of these mortar mixes reach 47MPa at 28 days, while the control mix reaches 53MPa. In addition, observing the compressive strengths at 90 days, the control mortar reaches 56MPa when the mortar mix replacing 10% by BBA of Puente Genil (10B-PGS) reaches 53 MPa, this resistance being 95% of the resistance presented by the control mortar. Figure 8 and figure 9 show the compressive and flexural strength.

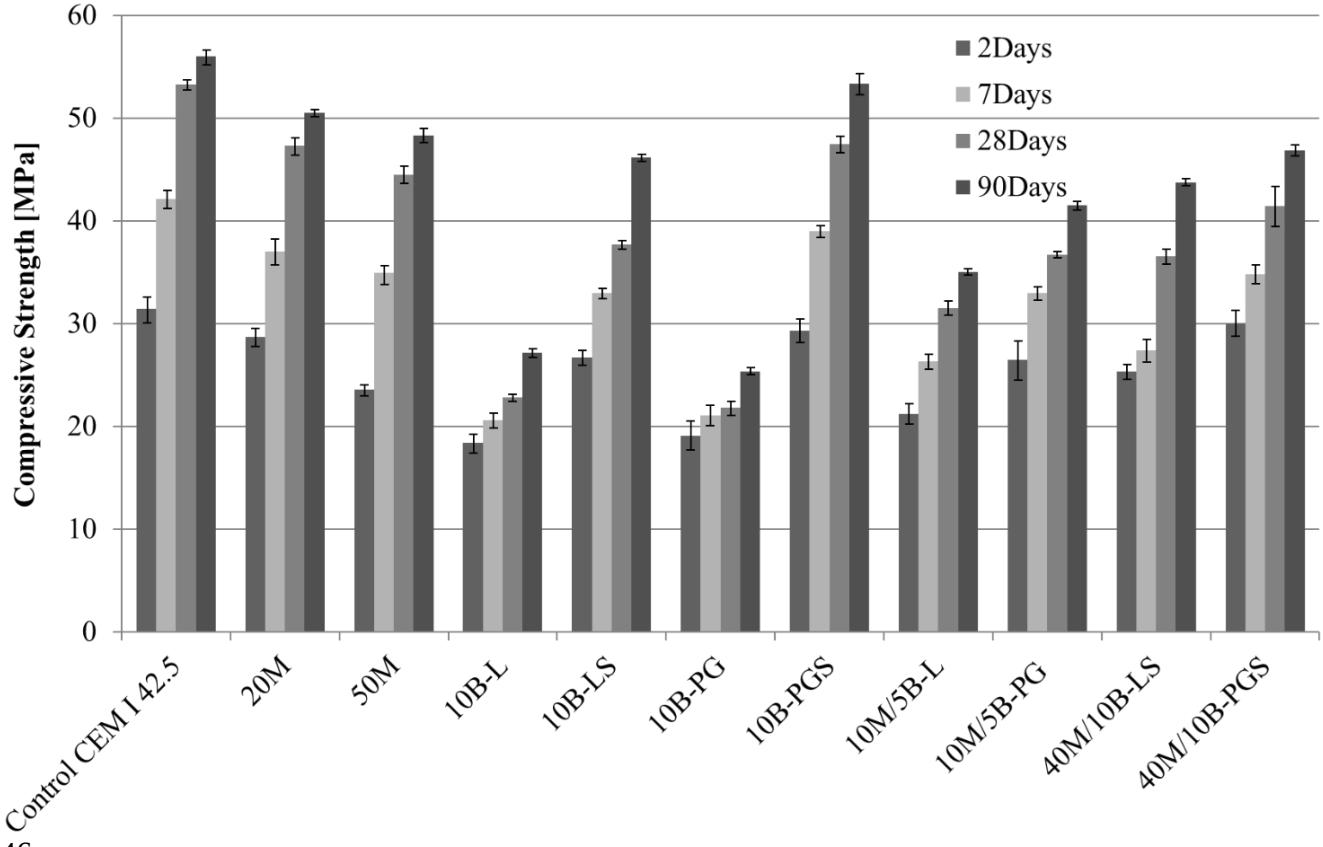

Figure 8. Compressive strength of mortar mixes.

Other studies value mixed recycled aggregate as a substitute for natural aggregate. Studies such as Saiz Martínez et al., 2016 [75] reach high substitution rates (50%, 75% and 100%). The results of this study in 50% substitution rate reach 21 MPa at 28 days. The study carried out by Heidari et al., 2018 [76] shows a substitution from 0% to 100% of the natural sand by recycled aggregate. Compared to this study, the drop in compression of a 20% substitution is negligible and the drop in strength when 50% is substituted is 20% of compression strength performance.

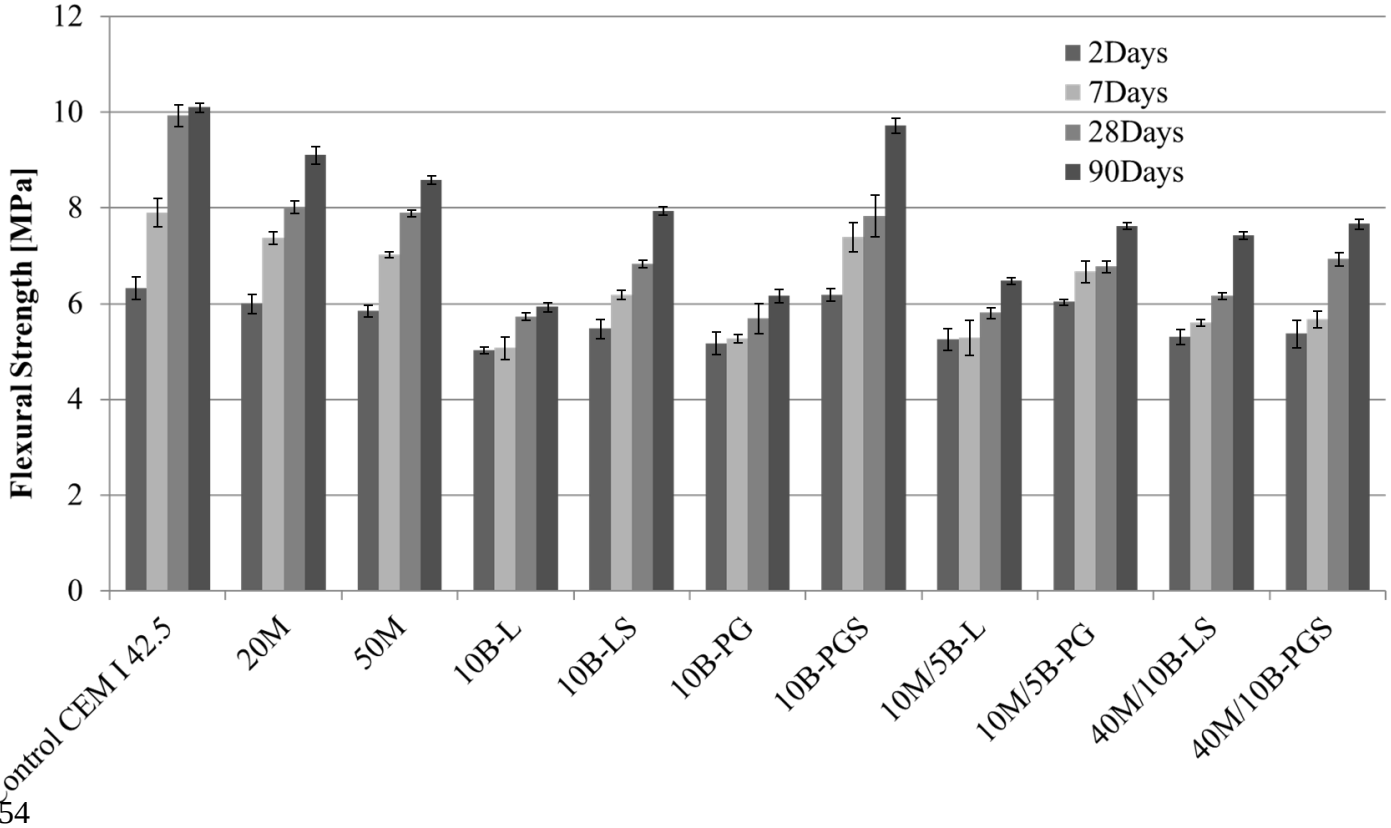

Figure 9. Flexural strength of mortar mixes.

In mixtures with a high substitution of 50% of the normalised natural sand, it is observed that the MRA reaches a strength of 44MPa and 48MPa at 28 days and 90 days, respectively. Both breaks at both 28 days and 90 days reach 86% of the strength of the conventional mortar mix. As discussed above, of the low-substitution mixes, the best mechanical behaviour was found to be that of the 10B-PGS mix. The hybrid substitution mix with the best mechanical performance is 40M/10B-PGS, reaching 77% of the compressive strength of the control mix at 28 days and 83% at 90 days. In figure 10, it can be observed the relative strength of each of the mortar mixes with respect to the strength of the conventional or control mortar. Other studies evaluating flexural strength show that there is an increase in flexural strength when recycled aggregates are included. Substitutions of 20% natural sand for recycled aggregate show an increase in flexural strength of 15% and substitutions of 50% natural sand for recycled aggregate show an increase of 30%. [76].

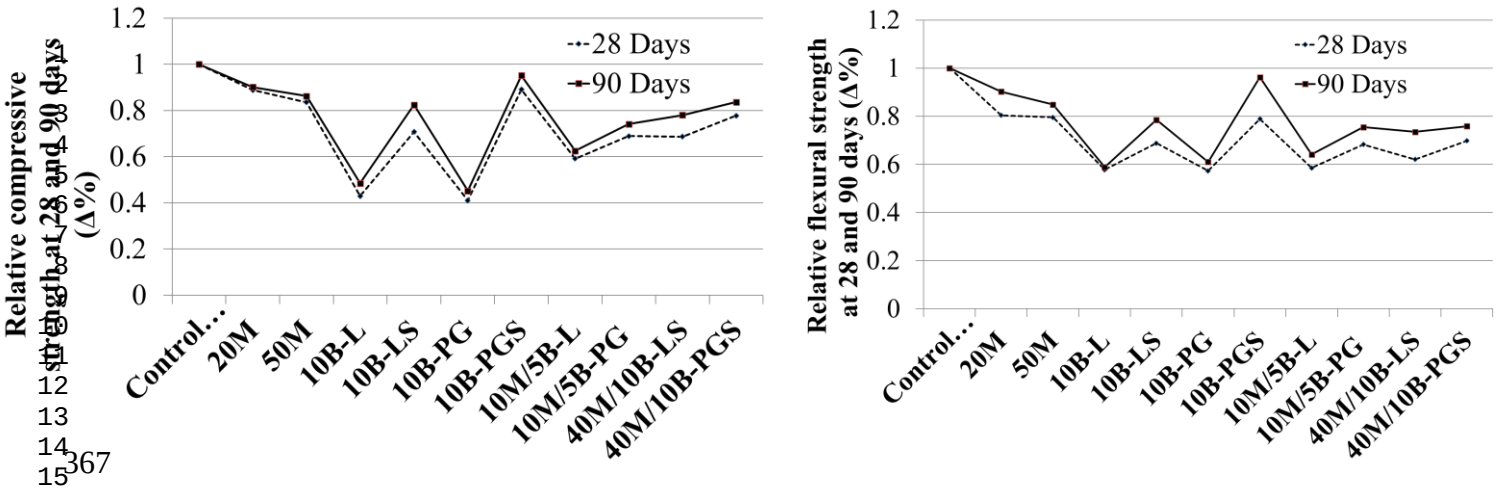

Figure 10. Relative strength with respect control mortar.

For mechanical flexural strengths, the mixtures with the best mechanical performance are the same as those for compression. At 90 days, 20MRA reaches 89% and 10B-PGS reaches 96% of the control mix strength. For mixes that include a high percentage of wastes, the mix with the highest flexural strength is 50M, reaching 85% with respect to the CEM I 42.5 control at 90 days. The best combination of waste is 40M/10B-PGS, reaching 75% of the strength of the control mix at 90 days. It should be noted that the high-substitution hybrid mortar with BBA from Linares (40M/10B-LS) also has a 74% flexural strength at 90 days.

Table 12. Increasing resistance from 28 days to 90 days.

Increasing resistance 28D→90D (%)	Control OPC	20M	50M	10B-L	10B-LS	10B-PG	10B-PGS	10M/5B-L	10M/5B-PG	40M/10B-LS	40M/10B-PGS
Compressive Strength	+4.9	+6.3	+7.8	+15.8	+18.4	+13.8	+11.0	+10.1	+11.6	+16.3	+11.6

Table 12 shows the growth of mechanical behavior in percentage between 28 days and 90 days. The mixtures that show a higher growth in this period of time are those that include biomass bottom ash with the ultrafine material removed. The compressive strength of the 10B-LS mix grows by 18.4%% and the 40M/10B-LS mix grows by 16.3% in the maturation process between 28 and 90

days.

4.2. Dimensional changes. Dry chamber and under water conditions.

Dimensional changes were measured throughout the curing process of the mortar mixes under study. With a micrometric precision comparator, measurements were made on the length variations in square section specimens of side 2cm and length 28.5cm. The measurements were taken at different stages of maturity, at 2, 7, 14, 28, 56, 72 and 90 days. In addition, to measure dimensional changes, all the mixtures were subjected to two curing environments. The cure environments are in the Dry Chamber and Under Water. The results of the dimensional changes are shown in figure 11.

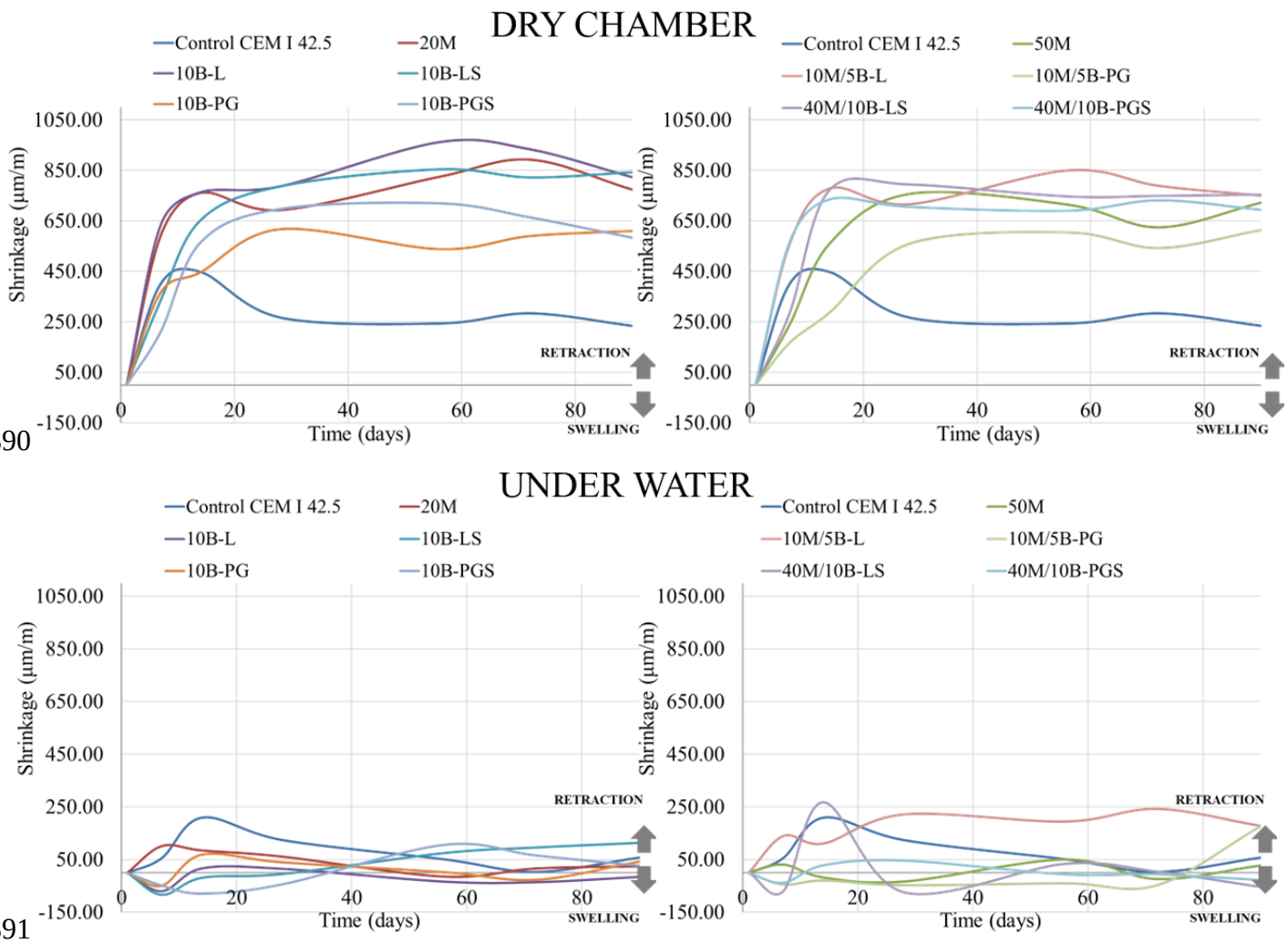

Figure 11. Dimensional changes of mortar mixes.

Figure 11 shows how the mixtures cured in the dry chamber undergo a greater dimensional change, retracting their size. It should be noted that the size stability of the mixtures cured in the dry chamber is reached at 28 days compared to those cured under water, which is reached at 56 days.

In the dry chamber curing environment, the mixtures with substituents present shrinkage between 600μm/m and 800μm/m, while the control mix, however, presents a shrinkage of 200μm/m. The mix with the highest shrinkage is 10B-LS, with 840μm/m at 90 days.

With respect to the mortar mixes that have been cured under water, the long-term dimensional change is small. The dimensional changes of all the mixes are between 60μm/m swelling and 180μm/m shrinkage. The mortar mix with the highest swelling is 10M/10B-LS and the one with the highest retraction is 10M/5B-PG. When compared with the control mix, it can be seen that both the progression of dimensional changes up to the stabilisation value and the shrinkage of the mix are in the range of 60μm/m swelling and 180μm/m retraction.

4.3. Hardened density and open porosity. UNE 83980:2014 [77].

Hardening density and accessible porosity tests were carried out for all mortar mixes. Open porosity is the volumen of air accessible, including cracks or pores. Several factors can influence the appearance of pores, such as curing, the age of the mix, the water-cement ratio or size, particle size distribution and nature of the aggregates [78]. The results obtained are presented in figure 12.

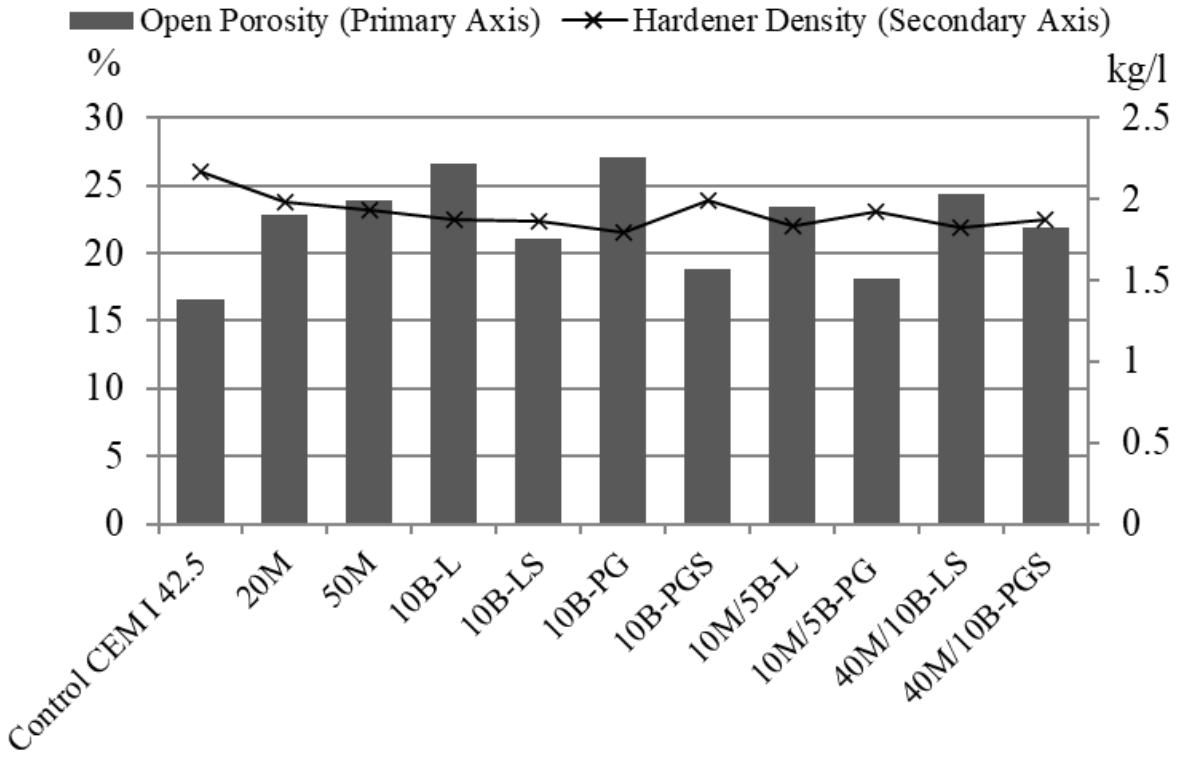

Figure 12. Open porosity and hardener density

It is observed that mixtures with higher density have a lower number of accessible pores. The Control CEM I 42.5, 10B-PGS and 10M/5B-PG mixtures have the lowest porosity and the highest density. It should be noted that, comparing mixtures with the same accessible porosity, the mixtures with MRA substitutes only have a higher density. BBA-PG and BBA-L materials are less dense than the MRA applied in this study. It is logical that mixtures containing BBA are less dense than mixtures containing MRA.

Mixtures containing BBA make the masonry mortars studied lighter. This causes a lower thermal and acoustic conductivity. [79]. Values of open porosity in façades mortars in other studies are between 15% and 30% [80].

4.4. Microproperties of hardened mortars

From all the mortar mixes studied, three of them with acceptable mechanical behaviour and high

replacement rates have been selected to analyse their microstructural properties. First of all, the mercury intrusion porosimetry test is presented, followed by a SEM analysis accompanied by XRD in which the pores and internal structures of the mortar mixes are observed.

4.4.1 Mercury Intrusion Porosimetry.

The Mercury intrusion porosimetry test was carried out on the mixes with 50% replacement of natural sand by recycled elements with better mechanical behaviour. The 50M, 40M/10BLS and 40M/10BPGS mortar mixes were included in this study. Figure 13 shows the distribution and specific pore volume of the above mentioned mixes.

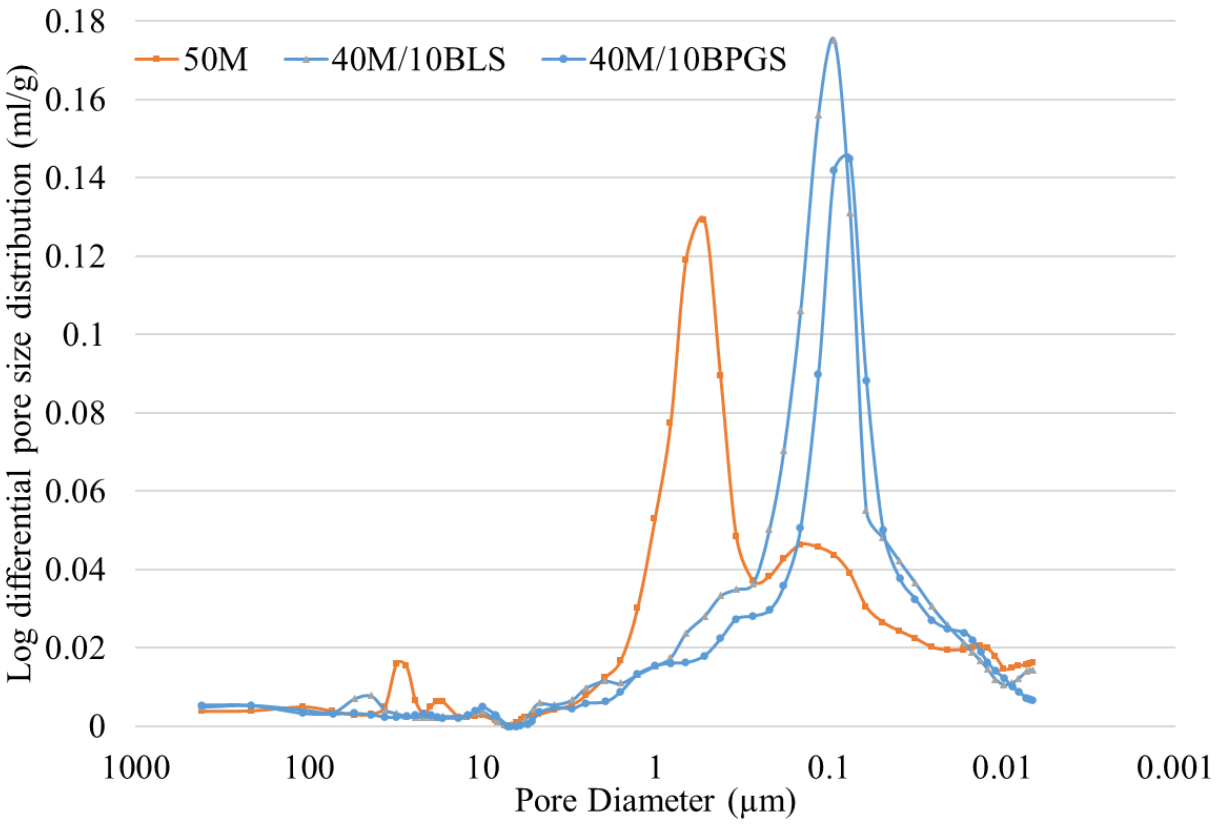

Figure 13. Mercury Intrusión Porosimetry of 50M, 40M/10BLS and 40M/10BPGS mortar mixes.

The mixtures containing BBA have a similar porosimetry, with a peak pore index at 0.1 µm. For the 50M mixture, a peak is found at 0.9 µm. Other studies using BBA show similar results with peaks in 0.1 µm in replacement grade of 30% and 50% [81]. Porosity is directly related to two

parameters, the particle size distribution and the amount of water added [82]. In mortar mixes with sand substitution rates higher than 10%, the consistency of the fresh mix changes considerably with respect to the control. To achieve the same workability, it is necessary to add more water to saturate the recycled element. With absorption rates of 19%-20% for BBA and 10% for MRA the water required to saturate the recycled materials is substantial and can create pores, and in order to avoid this the use of additives is necessary.

4.4.2 Scanning Electron Microscopy (SEM)

Mixtures with a 50% substitution of standard natural sand by recycled elements were analysed by scanning electron microscopy. Thanks to this test, the morphology of the hardened mortar and the shape and size of the particles within the cementitious matrix can be observed. All figures with BBA shows a diversity of particle sizes, typical of adding biomass ash to mortar mixes. [83, 84].

An element distribution analysis was carried out by energy dispersive spectroscopy (EDS), including phases with elements such as Si, Al, Ca O, or Fe.

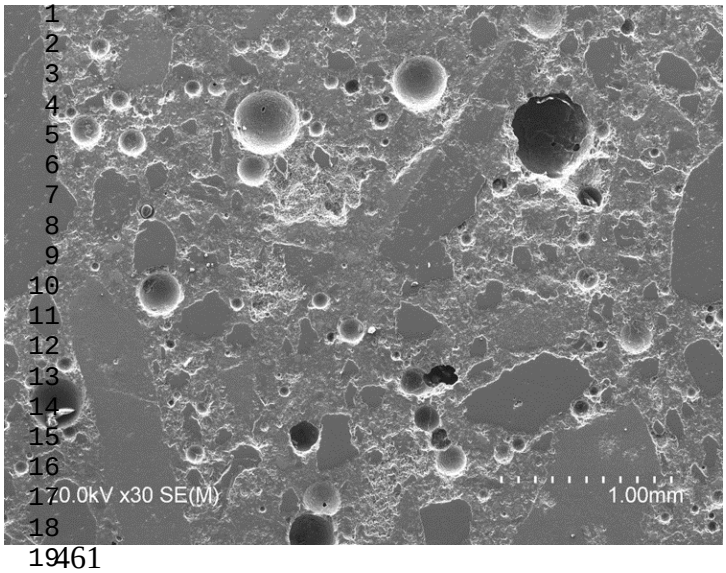

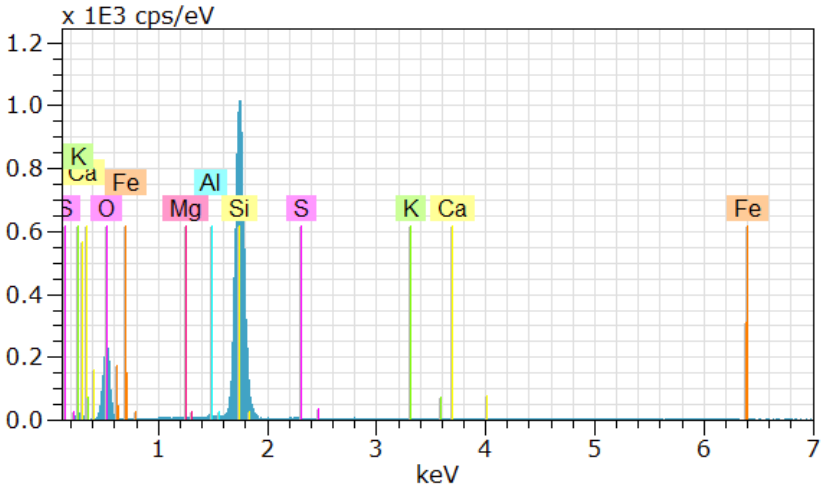

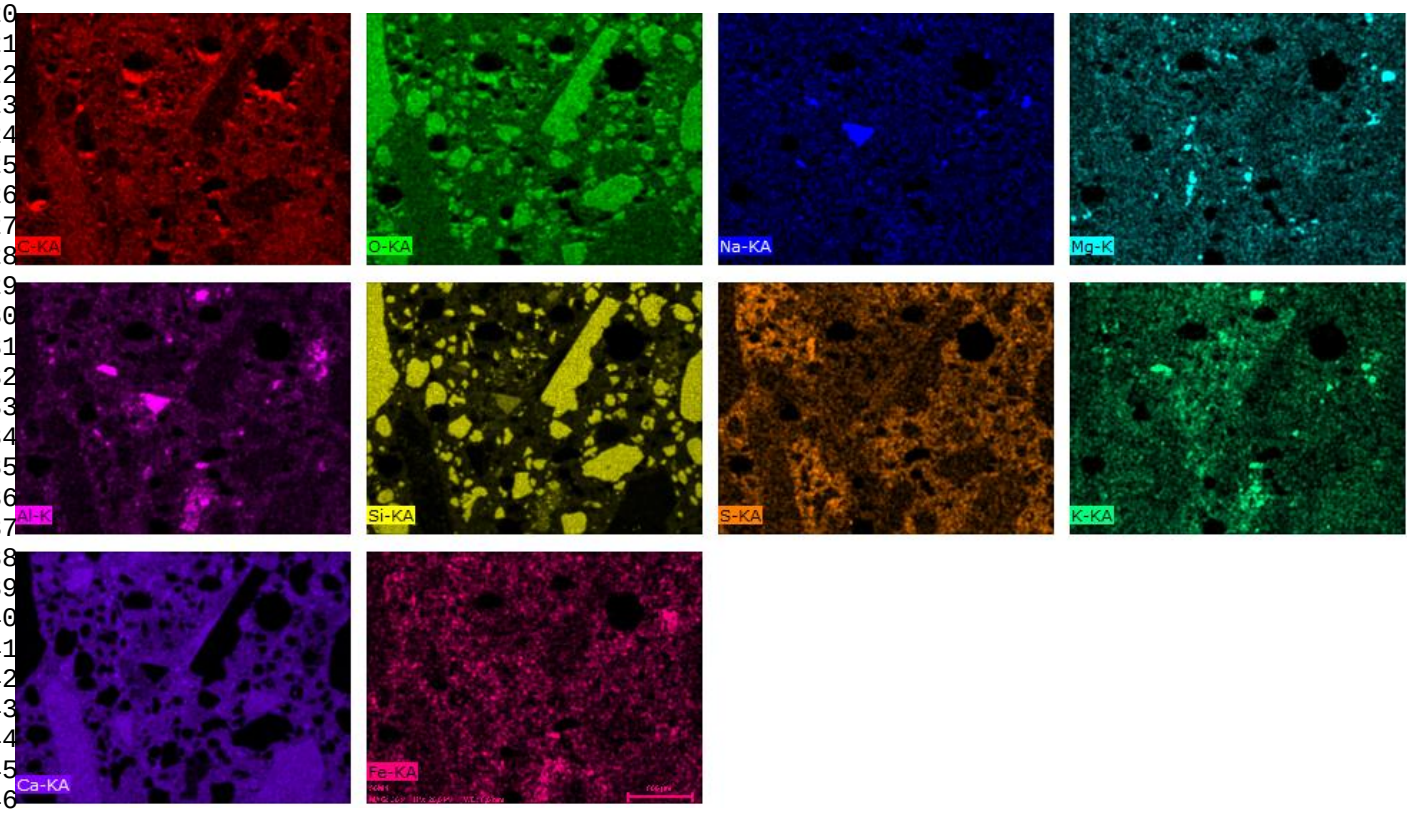

Figure 14. Elemental distribution map of the major elements and XRD of aluminosilicates in 50M mortar mix.

In the 50M mortar mix, it is observed that the silica and oxygen particles are located in the same zones of the mortar mix analysed, so that silica phases may be present, probably in the form of quartz. In addition, there are similar illuminated zones for carbon, oxygen and calcium, probably due to the presence of $CaCO_3$ phases; the compositions vary mainly in silica and calcium content.

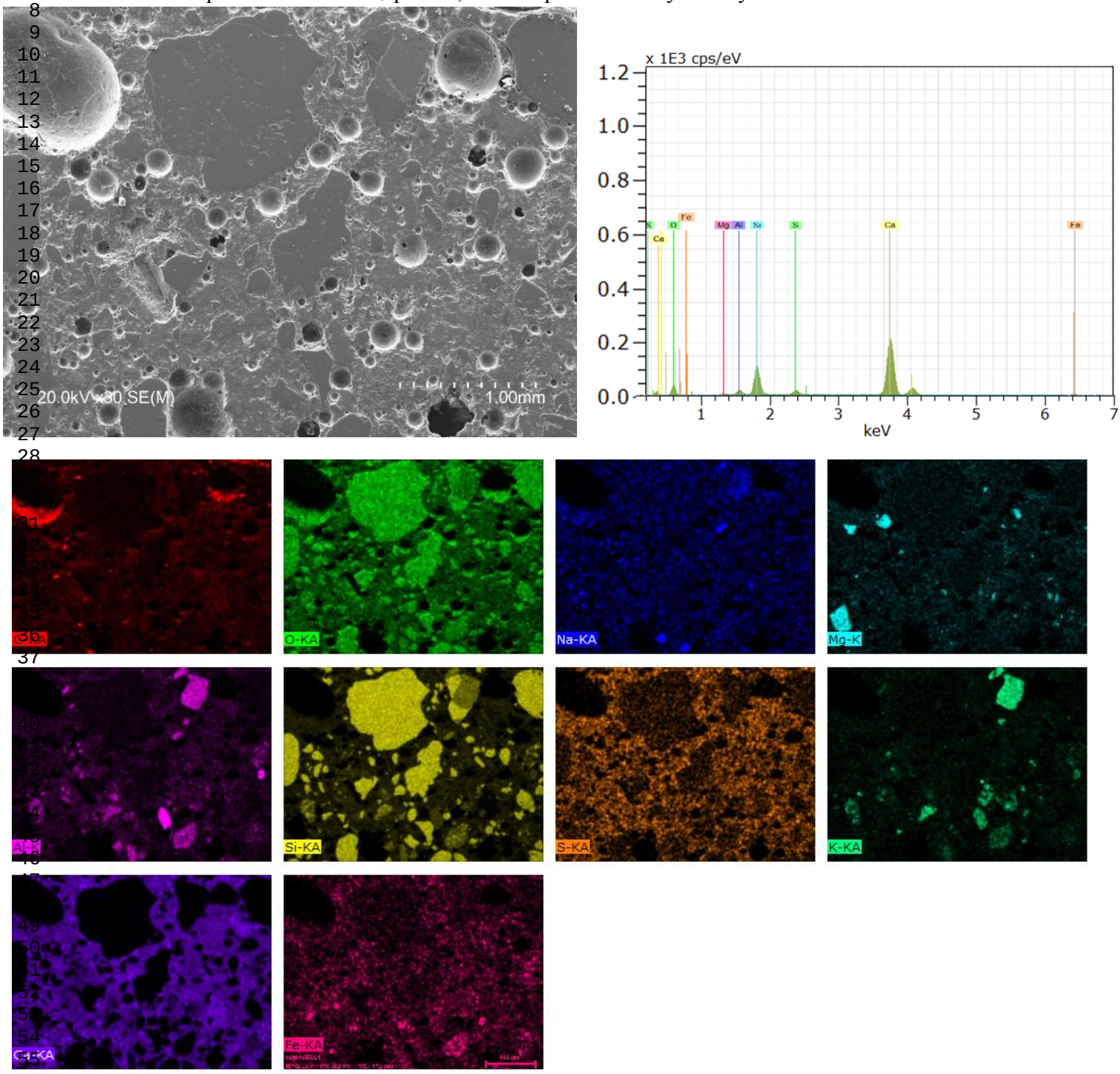

Figure 15. Elemental distribution map of the major elements and XRD of hydrated calcium silicates in 40M/10B-LS mortar mix.

The element distribution map shows that the amount of carbon is very localised, likely due to the presence of unburned elements [85] and the presence of elements with a high degree of alkalinity, such as potassium or sodium, is limited. The major elements observable in the SEM analysis of the 40M/10B-PGS mortar mix are silicon, oxygen and calcium, main components of calcite and quartz.

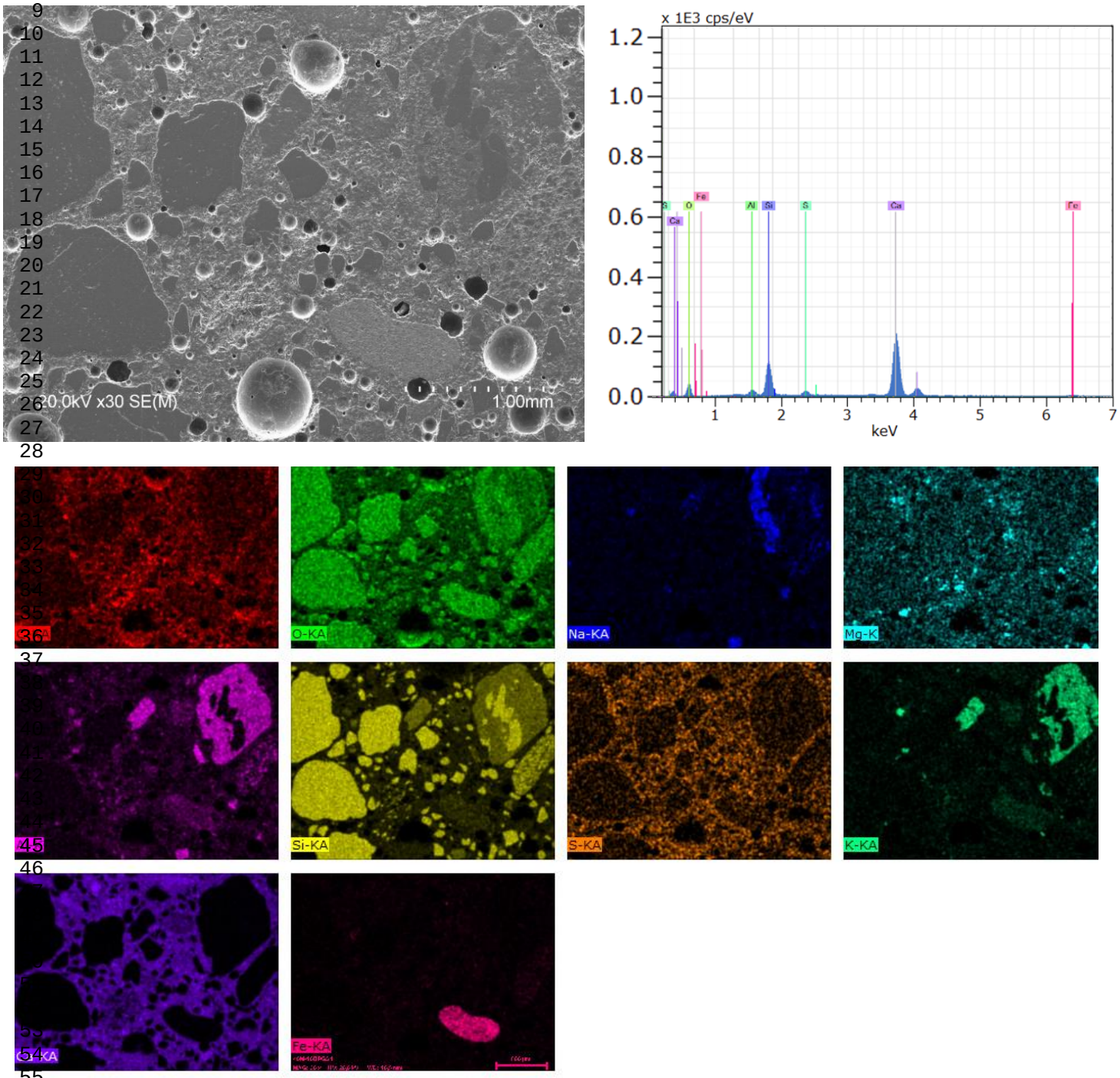

Figure 16. Elemental distribution map of the major elements and XRD of aluminosilicates in 40M/10B-PGS mortar mix.

It is observed that the presence of potassium is very accentuated in 50M mortar mix comparison with the analysed mixtures containing BBA, which may be due to the presence of feldspars, both from the phases contributed by the BBA and the MRA. However, hydration of potassium phases, which are normally found in the BBA, can produce undesirable internal structures [86]. A previous washing treatment could eliminate undesired alkaline salts like K_2O or MgO that affects directly durability and hydration process of mortar mixes [65].

A quantitative elemental analysis of the 50M, 40M/10B-LS and 40M/10B-PGS mortar samples is shown in table 13, related to figure 18.

Table 13. Quantification of elements via SEM of mortar mixes

%	50M					40M/10B-LS			40M/10B-PGS			
Element	**1**	**2**	**3**	**4**	**5**	**6**	**7**	**8**	**9**	**10**	**11**	**12**
SiO_2	58.67	10.79	14.62	2.83	83.63	94.45	19.65	19.51	59.38	59.26	23.82	23.32
Al_2O_3	20.25	1.81	3.30	0.01	1.28	2.35	3.24	3.34	22.19	22.27	2.67	5.28
CaO	4.99	84.62	78.20	94.60	14.64	0.58	69.63	69.55	0.53	0.59	66.04	63.54
Fe_2O_3	4.31	1.38	1.27	0.67	0.09	1.36	2.76	2.78	0.14	0.16	1.70	1.93
K_2O	0.12	0.42	1.67	0.16	0.10	0.97	2.01	1.94	16.97	16.94	0.47	0.31
Na_2O	10.56	0.00	0.00	0.00	0.00	0.00	0.00	0.00	0.79	0.78	0.00	0.00
SO_3	0.00	0.60	0.93	1.72	0.20	0.00	2.71	2.64	0.00	0.00	4.16	5.61

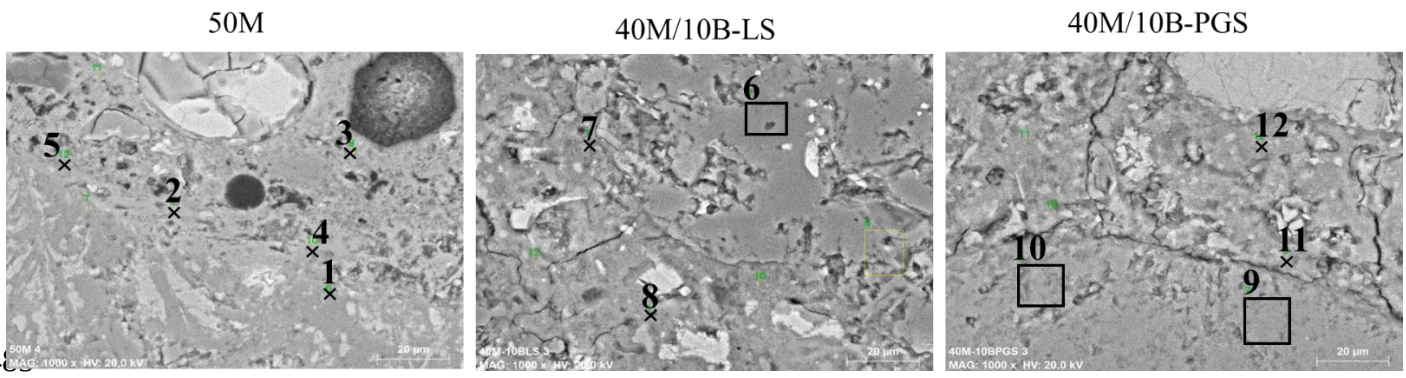

Figure 17. SEM pictures at 1000x magnification

It is observed that the majority elements in general are SiO_2, Al_2O_3 and CaO. There are also undesirable elements such as K_2O, Na_2O and SO_3. The existence of K_2O, possibly derived from introducing biomass [11], is more accentuated in points 9, 10 belonging to mortar 40M/10B-PGS.

There are studies that determine that the washing of the biomass bottom ash before introducing it into the mortar mixtures can considerably reduce the existence of potassium [87]. In the study by C. Famy et al. [88] the proportion of each element is related to possible crystals formed. Performing the analysis provided by this study, the existence of Portlandite occurs in points 2 and 3 of 50M, 7 and 8 of 10M/10B-LS and 11 and 12 of 40M/B-PGS. At the points where aluminum and silicon phases exist, we find aluminosilicates as points 1 of 50M and 8 and 9 of 40M/10B-PGS.

5. Conclusions

This study investigates the application of two types of processed waste, biomass bottom ash (BBA) and mixed recycled aggregates (MRA) to replace sand for the manufacture of mortars, and the most relevant conclusions reached are the following:

1.- When applying BBA and MRA with different processes instead of natural aggregates for the manufacture of mortars, lower densities are obtained in the final product. In addition, there is a greater demand for water due to the greater porosity of these materials, which must be adequately controlled to avoid excess water in the hardening process of the mixes.

2.- Different specific processes have been applied, mainly to the BBA, to eliminate in some cases the finest particles by sieving, which have thus obtained a very substantial improvement in the resistant properties of the manufactured mortars by increasing more than 100% of resistance improvement between the mixture 10P-GS and 10P-G, at the age of 28 days.

3.- Two types of BBA have been applied, since they came from two different origins, and one from MRA. It is demonstrated that it is possible to apply combinations of both processed residues, for the manufacture of mortars, applying the adequate contents of water and additives for its adequate performance.

4.- The increase in resistance achieved in the mixtures with BBA and MRA was much higher

between 28 and 90 days, compared to that presented by the control, due to the pozzolanic activity that these processed residues present, as demonstrated in previous works.

5.- Higher drying shrinkage values were obtained in the mortar mixtures in which BBA and MRA were applied.

Acknowledgements

This work is in the scope of the project *Development of ´Smart´ surfacing and repair Materials from low-carbon by products for more effective active and predictive safety. Advanced applications for Roads,* ***SMATCAR*** funded by the Minister of Science and Innovation of Spain. The authors also would like to thanks to the technical teams of the Eduardo Torroja Institute for Construction Science and the University of Cordoba.

Authors' contribution

Conceptualization, M. Rosales, J. Rosales; methodology, F. Agrela and J. Rosales.; investigation, M. Rosales, M. Cabrera and M.I. Sánchez de Rojas; data curation, M. Rosales, M.I. Sánchez de Rojas; writing—original draft preparation, M. Rosales, J. Rosales; writing—review and editing, M. Rosales, J. Rosales and M. Cabrera; supervision, F. Agrela and J. Rosales. All authors have read and agreed to the published version of the manuscript.

References

[1] M.A.B. Omer, T. Noguchi, A conceptual framework for understanding the contribution of building materials in the achievement of Sustainable Development Goals (SDGs), Sustainable Cities and Society 52 (2020) 101869.

[2] S. Eurostat, Generation of waste by economic activity, Eurostat Luxembourg, 2018.

[3] M.H.A. Nasir, A. Genovese, A.A. Acquaye, S.C.L. Koh, F. Yamoah, Comparing linear and circular supply chains: A case study from the construction industry, International Journal of Production Economics 183 (2017) 443-457.

[4] P. Thongkamsuk, K. Sudasna, T. Tondee, Waste generated in high-rise buildings construction:

A current situation in Thailand, Energy Procedia 138 (2017) 411-416.

[5] A. Gopinath, A. Bahurudeen, S. Appari, P. Nanthagopalan, A circular framework for the valorisation of sugar industry wastes: Review on the industrial symbiosis between sugar, construction and energy industries, Journal of Cleaner Production 203 (2018) 89-108.

[6] L.A. Akanbi, L.O. Oyedele, K. Omoteso, M. Bilal, O.O. Akinade, A.O. Ajayi, J.M. Davila Delgado, H.A. Owolabi, Disassembly and deconstruction analytics system (D-DAS) for construction in a circular economy, Journal of Cleaner Production 223 (2019) 386-396.

[7] P.S. REN21, Renewables 2017 global status report, Secretariat Renewable Energy Policy Network for the 21 (2017).

[8] I. Bioenergy, Brazil: Bioenergy policies and status of implementation, Paris. Retrieved from IEA website: https://www. ieabioenergy. com/wp-content/uploads/2018/10/CountryReport2018_Brazil_final. pdf, last accessed on 5(16) (2018) 2020.

[9] W. WBA, Global Bioenergy Statistics 2014, World Bioenergy Association (2014).

[10] J. Koppejan, S. Van Loo, The handbook of biomass combustion and co-firing, Routledge2012.

[11] M. Cabrera, J.L. Díaz-López, F. Agrela, J. Rosales, Eco-Efficient Cement-Based Materials Using Biomass Bottom Ash: A Review, Applied Sciences 10(22) (2020) 8026.

[12] D. Hoornweg, L. Thomas, What a waste: solid waste management in Asia, The World Bank1999.

[13] J. de Brito, F. Agrela, R.V. Silva, 1 - Construction and demolition waste, in: J. de Brito, F. Agrela (Eds.), New Trends in Eco-efficient and Recycled Concrete, Woodhead Publishing2019, pp. 1-22.

[14] R. L. S. Ferreira, M. A. S. Anjos, C. Maia, L. Pinto, A. R. G. de Azevedo, J. de Brito, Long-term analysis of the physical properties of the mixed recycled aggregate and their effect on the properties of mortars, Construction and Building Materials 274 (2021) 121796.

[15] S. Roque, C. Maia Pederneiras, C. Brazão Farinha, J. de Brito, R. Veiga, Concrete-based and mixed waste aggregates in rendering mortars, Materials 13(8) (2020) 1976.

[16] E.F. Ledesma, J.R. Jiménez, J. Ayuso, J.M. Fernández, J. de Brito, Maximum feasible use of recycled sand from construction and demolition waste for eco-mortar production – Part-I: ceramic masonry waste, Journal of Cleaner Production 87 (2015) 692-706.

[17] S. Jesus, C. Maia, C.B. Farinha, J. de Brito, R. Veiga, Rendering mortars with incorporation of very fine aggregates from construction and demolition waste, Construction and Building Materials 229 (2019) 116844.

[18] R.L. Ferreira, M.A. Anjos, A.K. Nóbrega, J.E. Pereira, E. Ledesma, The role of powder content of the recycled aggregates of CDW in the behaviour of rendering mortars, Construction and building materials 208 (2019) 601-612.

[19] J. Silva, J. de Brito, R. Veiga, Fine ceramics replacing cement in mortars Partial replacement of cement with fine ceramics in rendering mortars, Materials and Structures 41(8) (2008) 1333-1344.

[20] M. Rosales, J. Rosales, F. Agrela, M.I. Sánchez de Rojas, M. Cabrera, Design of a new eco-hybrid cement for concrete pavement, made with processed mixed recycled aggregates and olive biomass bottom ash as supplementary cement materials, Construction and Building Materials 358

(2022) 129417.

[21] M. Cabrera, A.P. Galvin, F. Agrela, M.G. Beltran, J. Ayuso, Reduction of leaching impacts by applying biomass bottom ash and recycled mixed aggregates in structural layers of roads, Materials 9(4) (2016) 228.

[22] M. Sarkkinen, K. Kujala, K. Kemppainen, S. Gehör, Effect of biomass fly ashes as road stabilisation binder, Road Materials and Pavement Design 19(1) (2018) 239-251.

[23] M.G. Beltrán, F. Agrela, A. Barbudo, J. Ayuso, A. Ramírez, Mechanical and durability properties of concretes manufactured with biomass bottom ash and recycled coarse aggregates, Construction and Building Materials 72 (2014) 231-238.

[24] R.C.E. Modolo, T. Silva, L. Senff, L.A.C. Tarelho, J.A. Labrincha, V.M. Ferreira, L. Silva, Bottom ash from biomass combustion in BFB and its use in adhesive-mortars, Fuel Processing Technology 129 (2015) 192-202.

[25] J. Rosales, M. Cabrera, M.G. Beltrán, M. López, F. Agrela, Effects of treatments on biomass bottom ash applied to the manufacture of cement mortars, Journal of Cleaner Production 154 (2017) 424-435.

[26] J. Rosales, M. Cabrera, M. Lopez-Alonso, J.L. Díaz-López, F. Agrela, 9 - Specialized concrete made of processed biomass ash: lightweight, self-compacting, and geopolymeric concrete, in: P.O. Awoyera, C. Thomas, M.S. Kirgiz (Eds.), The Structural Integrity of Recycled Aggregate Concrete Produced with Fillers and Pozzolans, Woodhead Publishing2022, pp. 199-239.

[27] R. Rajamma, L. Senff, M.J. Ribeiro, J.A. Labrincha, R.J. Ball, G.C. Allen, V.M. Ferreira, Biomass fly ash effect on fresh and hardened state properties of cement based materials, Composites Part B: Engineering 77 (2015) 1-9.

[28] AENOR, UNE-EN 196-1. Methods of Testing Cements—Part. 1: Determination of Mechanical Resistance, 2018.

[29] AENOR, UNE-EN 933-11/AC:2010. Tests for geometrical properties of aggregates - Part 11: Classification test for the constituents of coarse recycled aggregate, 2009.

[30] S. Ihobe, Usos de áridos reciclados mixtos procedentes de Residuos de Construcción y Demolición, Pais Vasco: Ihobe SA (2011).

[31] C. Medina, W. Zhu, T. Howind, M.I.S. de Rojas, M. Frías, Influence of mixed recycled aggregate on the physical–mechanical properties of recycled concrete, Journal of cleaner production 68 (2014) 216-225.

[32] G. Bianchini, E. Marrocchino, R. Tassinari, C. Vaccaro, Recycling of construction and demolition waste materials: a chemical–mineralogical appraisal, Waste Management 25(2) (2005) 149-159.

[33] C. Ulsen, H. Kahn, G. Hawlitschek, E.A. Masini, S.C. Angulo, Separability studies of construction and demolition waste recycled sand, Waste Management 33(3) (2013) 656-662.

[34] AENOR, UNE-EN 1097-6. Tests for mechanical and physical properties of aggregates - Part 6: Determination of particle density and water absorption, 2014.

[35] AENOR, UNE 146404. Aggregates for concrete. Determination of the coefficient of friability of the sands, 2018.

[36] AENOR, UNE-EN 933-8:2012+A1:2015. ests for geometrical properties of aggregates - Part 8: Assessment of fines - Sand equivalent test, 2012.

[37] AENOR, UNE 103204. Organic matter content of a soil by the potassium permanganate method., 2019.

[38] AENOR, UNE-EN 1744-1:2010+A1:2013. Tests for chemical properties of aggregates - Part 1: Chemical analysis, 2010.

[39] J. Pacheco, J. de Brito, Recycled aggregates produced from construction and demolition waste for structural concrete: Constituents, properties and production, Materials 14(19) (2021) 5748.

[40] P.S. Martínez, M.G. Cortina, F.F. Martínez, A.R. Sánchez, Comparative study of three types of fine recycled aggregates from construction and demolition waste (CDW), and their use in masonry mortar fabrication, Journal of cleaner production 118 (2016) 162-169.

[41] M. González Cortina, P. Saiz Martínez, F. Martínez, C. Viñas Arrebola, Use of concrete recycled aggregates as a raw material in lightweight mortar fabrication, (2017).

[42] I. Vegas, J.A. Ibañez, A. Lisbona, A.S. De Cortazar, M. Frías, Pre-normative research on the use of mixed recycled aggregates in unbound road sections, Construction and Building Materials 25(5) (2011) 2674-2682.

[43] T.T. Kien, L.T. Thanh, P.V. Lu, Utilisation of construction demolition waste as stabilised materials for road base applications, The International Conference on Sustainable Built Environment for Now and the Future. Hanoi, 2013, p. 27.

[44] R. Silva, J. De Brito, R. Dhir, Use of recycled aggregates arising from construction and demolition waste in new construction applications, Journal of Cleaner Production 236 (2019) 117629.

[45] A. Juan-Valdés, D. Rodriguez-Robles, J. Garcia-Gonzalez, M.I.S. de Rojas Gómez, M.I. Guerra-Romero, N. De Belie, J.M. Morán-del Pozo, Mechanical and microstructural properties of recycled concretes mixed with ceramic recycled cement and secondary recycled aggregates. A viable option for future concrete, Construction and Building Materials 270 (2021) 121455.

[46] M. Rosales, J. Rosales, F. Agrela, M.S. de Rojas, M. Cabrera, Design of a new eco-hybrid cement for concrete pavement, made with processed mixed recycled aggregates and olive biomass bottom ash as supplementary cement materials, Construction and Building Materials 358 (2022) 129417.

[47] M. Nagao, K. Kobayashi, T. Hori, Y. Li, T. Hibino, Humidity driven transition from insulator to ionic conductor in Portland cement, Materials 12(22) (2019) 3701.

[48] M. Berra, T. Mangialardi, A.E. Paolini, Reuse of woody biomass fly ash in cement-based materials, Construction and Building Materials 76 (2015) 286-296.

[49] E. Arif, M.W. Clark, N. Lake, Sugar cane bagasse ash from a high efficiency co-generation boiler: Applications in cement and mortar production, Construction and Building Materials 128 (2016) 287-297.

[50] M. Hinojosa, A. Galvín, F. Agrela, M. Perianes, A. Barbudo, Potential use of biomass bottom ash as alternative construction material: Conflictive chemical parameters according to technical regulations, Fuel 128 (2014) 248-259.

[51] L. Munkholm, Soil friability: A review of the concept, assessment and effects of soil properties and management, Geoderma 167 (2011) 236-246.

[52] R. García, C. Pizarro, A. Álvarez, A.G. Lavín, J.L. Bueno, Study of biomass combustion wastes, Fuel 148 (2015) 152-159.

[53] L.B. Andrade, J. Rocha, M. Cheriaf, Evaluation of concrete incorporating bottom ash as a natural aggregates replacement, Waste Management 27(9) (2007) 1190-1199.

[54] M. Cabrera, A.P. Galvin, F. Agrela, M.D. Carvajal, J. Ayuso, Characterisation and technical feasibility of using biomass bottom ash for civil infrastructures, Construction and Building Materials 58 (2014) 234-244.

[55] A.P. Galvín, A. López-Uceda, M. Cabrera, J. Rosales, J. Ayuso, Stabilization of expansive soils with biomass bottom ashes for an eco-efficient construction, Environmental Science and Pollution Research 28(19) (2021) 24441-24454.

[56] M.G. Beltrán, A. Barbudo, F. Agrela, J.R. Jiménez, J. de Brito, Mechanical performance of bedding mortars made with olive biomass bottom ash, Construction and Building Materials 112 (2016) 699-707.

[57] AENOR, UNE 146513. Test for aggregates. Determination of the potential reactivity of aggregates. Chemical method. Determination of the alkali-carbonate reactivity., 2018.

[58] I. Sims, A.B. Poole, Alkali-aggregate reaction in concrete: A world review, CRC Press2017.

[59] M.B. Santos, J. de Brito, A.S. Silva, A. Hawreen, Evaluation of alkali-silica reaction in recycled aggregates: The applicability of the mortar bar test, Construction and Building Materials 299 (2021) 124250.

[60] S. Maschio, G. Tonello, L. Piani, E. Furlani, Fly and bottom ashes from biomass combustion as cement replacing components in mortars production: Rheological behaviour of the pastes and materials compression strength, Chemosphere 85(4) (2011) 666-671.

[61] AENOR, UNE-EN 12457-3. Characterisation of waste - Leaching - Compliance test for leaching of granular waste materials and sludges - Part 3: Two stage batch test at a liquid to solid ratio of 2 l/kg and 8 l/kg for materials with high solid content and with particle size below 4 mm (without or with size reduction), 2003.

[62] L.F. Roca, J. Moral, J.R. Viruega, A. Ávila, R. Oliveira, A. Trapero, Copper fungicides in the control of olive diseases, Olea 26 (2007) 48-50.

[63] C. Gessler, I. Pertot, M. Perazzolli, Plasmopara viticola: a review of knowledge on downy mildew of grapevine and effective disease management, Phytopathologia Mediterranea 50(1) (2011) 3-44.

[64] S. Ihobe, Usos de áridos reciclados mixtos procedentes de Residuos de Construcción y Demolición, Pais Vasco: Ihobe SA, 2011.

[65] B. Carrasco, N. Cruz, J. Terrados, F. Corpas, L. Pérez, An evaluation of bottom ash from plant biomass as a replacement for cement in building blocks, Fuel 118 (2014) 272-280.

[66] V. Sklivaniti, P. Tsakiridis, N. Katsiotis, D. Velissariou, N. Pistofidis, D. Papageorgiou, M. Beazi, Valorisation of woody biomass bottom ash in Portland cement: A characterization and hydration study, Journal of environmental chemical engineering 5(1) (2017) 205-213.

[67] S.A. Zareei, F. Ameri, N. Bahrami, Microstructure, strength, and durability of eco-friendly concretes containing sugarcane bagasse ash, Construction and Building Materials 184 (2018) 258-268.

[68] M. Cruz-Yusta, I. Mármol, J. Morales, L. Sánchez, Use of olive biomass fly ash in the preparation of environmentally friendly mortars, Environmental science & technology 45(16) (2011) 6991-6996.

[69] S. Onutai, T. Osugi, T. Sone, Alumino-Silicate Structural Formation during Alkali-Activation of Metakaolin: In-Situ and Ex-Situ ATR-FTIR Studies, Materials 16(3) (2023) 985.

[70] V.S. Ramachandran, R.M. Paroli, J.J. Beaudoin, A.H. Delgado, Handbook of thermal analysis of construction materials, William Andrew2002.

[71] R.E. Grim, Clay mineralogy, LWW1953.

[72] J. Dweck, P.M. Buchler, A.C.V. Coelho, F.K. Cartledge, Hydration of a Portland cement blended with calcium carbonate, Thermochimica acta 346(1-2) (2000) 105-113.

[73] E. Stepkowska, J. Blanes, F. Franco, C. Real, J. Pérez-Rodrıguez, Phase transformation on heating of an aged cement paste, Thermochimica acta 420(1-2) (2004) 79-87.

[74] S. Gunasekaran, G. Anbalagan, Thermal decomposition of natural dolomite, Bulletin of Materials Science 30(4) (2007) 339-344.

[75] P. Saiz Martínez, M. González Cortina, F. Fernández Martínez, A. Rodríguez Sánchez, Comparative study of three types of fine recycled aggregates from construction and demolition waste (CDW), and their use in masonry mortar fabrication, Journal of Cleaner Production 118 (2016) 162-169.

[76] A. Heidari, M. Hashempour, H. Javdanian, M. Karimian, Investigation of mechanical properties of mortar with mixed recycled aggregates, Asian Journal of Civil Engineering 19(5) (2018) 583-593.

[77] AENOR, UNE 83980. Concrete durability. Test methods. Determination of the water absorption, density and accessible porosity for water in concrete., 2014.

[78] I. Papayianni, M. Stefanidou, Strength–porosity relationships in lime–pozzolan mortars, Construction and Building Materials 20(9) (2006) 700-705.

[79] L. Silva, R. Ribeiro, J. Labrincha, V. Ferreira, Role of lightweight fillers on the properties of a mixed-binder mortar, Cement and Concrete Composites 32(1) (2010) 19-24.

[80] I. Flores‐Colen, L. Silva, J. de Brito, V. Peixoto de Freitas, In‐service parameters from façade rendering mortars: Bulk density and open porosity determined from samples collected in situ, Structural Survey 28(1) (2010) 17-27.

[81] M. Wyrzykowski, S. Ghourchian, S. Sinthupinyo, N. Chitvoranund, T. Chintana, P. Lura, Internal curing of high performance mortars with bottom ash, Cement and Concrete Composites 71 (2016) 1-9.

[82] A.B. Ayobami, Performance of wood bottom ash in cement-based applications and comparison with other selected ashes: Overview, Resources, Conservation and Recycling 166 (2021) 105351.

[83] N.S. Trivedi, S.A. Mandavgane, S. Mehetre, B.D. Kulkarni, Characterization and valorization of biomass ashes, Environmental Science and Pollution Research 23 (2016) 20243-20256.

[84] N.S. Trivedi, S.A. Mandavgane, A. Chaurasia, Characterization and valorization of biomass char: a comparison with biomass ash, Environmental Science and Pollution Research 25 (2018) 3458-3467.

[85] A.K. James, R.W. Thring, S. Helle, H.S. Ghuman, Ash management review—applications of biomass bottom ash, Energies 5(10) (2012) 3856-3873.

[86] T.A. Santos, J.S.A. Neto, M.S. Cilla, D.V. Ribeiro, Influence of the Content of Alkalis (Na 2

O and K 2 O), MgO, and SO 3 Present in the Granite Rock Fine in the Production of Portland Clinker, Journal of Materials in Civil Engineering 34(3) (2022) 04021464.

[87] R. Modolo, V. Ferreira, L. Tarelho, J. Labrincha, L. Senff, L. Silva, Mortar formulations with bottom ash from biomass combustion, Construction and Building Materials 45 (2013) 275-281.

[88] C. Famy, A. Brough, H. Taylor, The CSH gel of Portland cement mortars: Part I. The interpretation of energy-dispersive X-ray microanalyses from scanning electron microscopy, with some observations on CSH, AFm and AFt phase compositions, Cement and Concrete Research 33(9) (2003) 1389-1398.